AD-A175 441 A NUMERICAL INVESTIGATION OF FINITE - VOLUME TECHNIQUES 1/1
USING THE INVISCI..(U) AIR FORCE ARMAMENT LAB EGLIN AFB
FL J S MOUNTS ET AL. OCT 86 AFATL-TR-86-66
UNCLASSIFIED SBI-AD-E801 412 F/G 20/4 NL

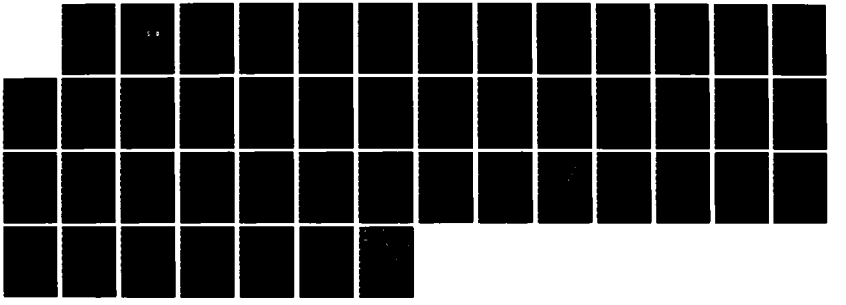

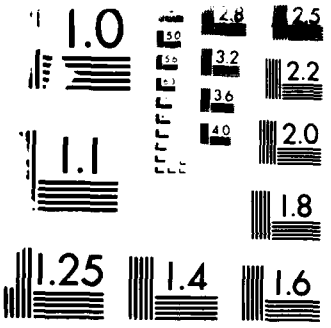
1.0
1.1
1.25
1.4
1.6
1.8
2.0
2.2
2.5
2.8
3.2
3.6
4.0

AFATL-TR-86-66

A Numerical Investigation of Finite-Volume Techniques Using the Inviscid Burgers Equation

Jon S Mounts, 1Lt, USAF
Montgomery C. Hughson, 2Lt, USAF
Dave M Belk

AERODYNAMICS BRANCH
AEROMECHANICS DIVISION

OCTOBER 1986

INTERIM REPORT FOR PERIOD OCTOBER 1985 - SEPTEMBER 1986

APPROVED FOR PUBLIC RELEASE; DISTRIBUTION UNLIMITED

AIR FORCE ARMAMENT LABORATORY
Air Force Systems Command ▮ United States Air Force ▮ Eglin Air Force Base, Florida

REPORT DOCUMENTATION PAGE

1a. REPORT SECURITY CLASSIFICATION Unclassified	1b. RESTRICTIVE MARKINGS
2a. SECURITY CLASSIFICATION AUTHORITY N/A	3. DISTRIBUTION/AVAILABILITY OF REPORT Approved for public release; distribution is unlimited.
2b. DECLASSIFICATION/DOWNGRADING SCHEDULE N/A	
4. PERFORMING ORGANIZATION REPORT NUMBER(S) AFATL-TR-86-66	5. MONITORING ORGANIZATION REPORT NUMBER(S)
6a. NAME OF PERFORMING ORGANIZATION Air Force Armament Laboratory Aerodynamics Branch 6b. OFFICE SYMBOL (If applicable) AFATL/FXA	7a. NAME OF MONITORING ORGANIZATION Air Force Armament Laboratory Aeromechanics Division
6c. ADDRESS (City, State and ZIP Code) Eglin AFB, FL 32542-5434	7b. ADDRESS (City, State and ZIP Code) Eglin AFB, FL 32542-5434
8a. NAME OF FUNDING/SPONSORING ORGANIZATION N/A 8b. OFFICE SYMBOL (If applicable)	9. PROCUREMENT INSTRUMENT IDENTIFICATION NUMBER N/A
8c. ADDRESS (City, State and ZIP Code) N/A	10. SOURCE OF FUNDING NOS. PROGRAM ELEMENT NO.: 62602F PROJECT NO.: 2567. TASK NO.: 03 WORK UNIT NO.: 08

11. TITLE (Include Security Classification)
A Numerical Investigation of Finite-Volume Techniques Using the Inviscid Burgers Equation (U

12. PERSONAL AUTHOR(S)
Jon S. Mounts, Montgomery C. Hughson, and Dave M. Belk

13a. TYPE OF REPORT	13b. TIME COVERED	14. DATE OF REPORT (Yr., Mo., Day)	15. PAGE COUNT
Interim	FROM Oct 85 TO Sep 86	October 1986	48

16. SUPPLEMENTARY NOTATION
None

17. COSATI CODES		
FIELD	GROUP	SUB. GR.
01	01	

18. SUBJECT TERMS (Continue on reverse if necessary and identify by block number)
Numerical Method
Finite-Volume Techniques
Burgers Equation

19. ABSTRACT (Continue on reverse if necessary and identify by block number)

A numerical investigation of finite-volume techniques using the inviscid Burgers equation was conducted. An explicit, second-order, one-sided, or upwind differencing scheme developed by Warming and Beam was used. First, the difference scheme was analyzed for consistency, stability, convergence, phase and dispersion error, and artificial dissipation. Then, various combinations of finite-volume and extrapolation techniques were tested and conclusions and recommendations for their use were formulated.

20. DISTRIBUTION/AVAILABILITY OF ABSTRACT	21. ABSTRACT SECURITY CLASSIFICATION
UNCLASSIFIED/UNLIMITED ☒ SAME AS RPT. ☒ DTIC USERS ☐	Unclassified

22a. NAME OF RESPONSIBLE INDIVIDUAL	22b. TELEPHONE NUMBER (Include Area Code)	22c. OFFICE SYMBOL
JON S. MOUNTS	(904) 882-3124	FXA

PREFACE

This report was prepared by Jon S. Mounts, Montgomery C. Hughson, and Dave M. Belk of the Computational Fluid Dynamics Section, Aerodynamics Branch, Aeromechanics Division, Air Force Armament Laboratory, Eglin AFB, Florida. The work was performed under work unit 25670308 during the fiscal year period from 1 October 1985 to 30 September 1986.

This report presents the investigation of finite-volume techniques employed in current Euler codes, in use in the Computational Fluid Dynamics Section.

(The reverse of this page is blank)

TABLE OF CONTENTS

LIST OF FIGURES

LIST OF SYMBOLS AND ABBREVIATIONS

U_i	Velocity in the x Direction
F	Flux
C	Constant Wave Speed
FDE	Finite Difference Equation
PDE	Partial Differential Equation
n	Time Step
i	Spatial Step (x Direction)
Δt	Change in Time Step (Incremental)
Δx	Change in Spatial Step (Incremental)
ν	Courant Number
ϕ	Phase Angle of the Amplification Factor
γ	Wave Number ($kj\Delta x$)
$\|G\|$	Amplification Factor
A^o	Initial Amplitude of the Fourier Component

(The reverse of this page is blank)

SECTION I

INTRODUCTION

Researchers in aerodynamic analysis and design have turned to numerical techniques, with the advent of the supercomputer (Cyber 205, Cray X-MP, Cray 2, etc.), to solve for the fluid flow about weapon/store configurations. Current aerodynamic research at the Air Force Armament Laboratory (AFATL) is aimed at solving the equations that govern fluid flow problems using a variety of approximation techniques. The governing partial differential equations (PDE) form a nonlinear system which must be solved for the unknown pressures, densities, temperatures, and velocities to yield the aerodynamic characteristics for a given weapon/store configuration at specific flight conditions.

To obtain a thorough approximation for the flow field about a configuration, we must solve the complete Navier-Stokes equations. However, due to limitations placed on researchers by current computer systems (time and storage), certain simplifying assumptions must be made to obtain results. By assuming an inviscid, adiabatic flow field (dropping viscous and heat transfer terms), we obtain the Euler equations. Results obtained from a solution of the Euler equations are particularly useful in preliminary design work where information on pressure alone is desired. These equations are also of interest because they incorporate many major fluid dynamics elements such as internal discontinuities (shock waves and contact surfaces). The Euler equations govern the motion of inviscid, non-heated gas and have different numerical characteristics in different flow regimes. For steady problems, the equations are elliptic in subsonic flow and hyperbolic in supersonic flow (Reference 1).

Research at AFATL is aimed at solving the three dimensional Euler equations to approximate the flow about arbitrarily-shaped weapon/store configurations. This research is accomplished using various implicit and explicit finite-difference and finite-volume techniques. Currently this work has lead to an analysis of two explicit, finite-volume procedures for solving the Euler equations. To help in this analysis of the numerical characteristics inherent to the two approaches, a single equation serving as a numerical analog to the Euler equations has been found. The inviscid Burgers equation (nonlinear wave equation) serves as this simple nonlinear analog to aid in our understanding of these techniques (Appendix A) (Reference 1).

SECTION II

UPWIND SCHEME

Several numerical techniques have been developed that will solve the partial differential equations that govern fluid flow, heat transfer, and combustion problems. These methods can be either explicit or implicit, central difference or upwind, single or multi-step, and first- or second-order accurate.

An explicit, second-order, one-sided, or upwind difference scheme for the numerical solution of hyperbolic systems has been developed by Warming and Beam (Reference 2). There are several advantages to the use of the Upwind schemes.

(1) One-sided schemes are often desirable along both fixed external boundaries and along moving internal boundaries (such as shocks), where a spatially centered scheme would require one or more points inside or across the boundary.

(2) An explicit, second-order upwind scheme can have twice the stability bound of a symmetric scheme using the same number of spatial grid points.

(3) The dissipative-dispersive properties of an upwind scheme are superior to those of a symmetric scheme.

(4) Switching schemes across a discontinuity can reduce the spurious oscillations usually associated with a second-order accurate shock-capturing technique. Warming and Beam's goal was to develop a hybrid scheme which exploits the advantages of a second-order upwind scheme for aerodynamic flows. This multi-step procedure applied to the inviscid Burgers equation is shown as follows:

Predictor:
$$\overline{U_i^{n+1}} = U_i^n - \frac{\Delta t}{\Delta x}\Delta F_i^n \tag{1a}$$

Corrector:
$$U_i^n = U_{i-\frac{1}{2}}^n + \overline{U_i^{n+1}} - \frac{\Delta t}{2\Delta x}\Delta \overline{F_i^{n+1}} - \frac{\Delta t}{2\Delta x}\Delta^2 \overline{F_i^{n+1}} \tag{1b}$$

where;
$$\Delta F_i = F_i - F_{i-1}. \tag{2}$$

A thorough error analysis has been performed on the Upwind scheme to aid in our understanding of the numerical characteristics inherent to this technique (Appendix B). This analysis includes consistency, convergence, numerical stability, phase and dispersion error, and artificial dissipation (Reference 3).

SECTION III

FINITE-VOLUME APPROACHES

For our research in computational aerodynamics, we have settled on the finite-volume (FV) approach, as opposed to the finite-difference (FD) method, to solve for the physics of the flow about a weapon/store configuration. Fundamentally, the primary difference between the two methods is that for the FV approach we solve for the flux at the face of a cell; the FD approach solves for the flux at the center of the cell (Figure 1). To accomplish this FV technique we must extrapolate either the flux or the dependent variable from the center of the cell to the face of the cell. The advantage to using the FV method is that, inherent to the approach, the conservative property of the PDE is fully maintained.

1. EXTRAPOLATION TECHNIQUES

As mentioned above, there are two extrapolation techniques that must be studied to determine which yields the optimum results. The flux term is $U(i)^2/2$ where the dependent variable is $U(i)$. For the upwind scheme, extrapolating the flux yields

$$2\,(U(i)^2/2) - (U(i-1)^2/2) \quad \text{or} \tag{3}$$

$$2\,(U(i+1)^2/2) - (U(i+2)^2/2)$$

depending on the direction of the flow of information. When extrapolating the dependent variable for the same inviscid Burgers equation, we get;

$$(2U(i) - U(i-1))^2/2 \quad \text{or} \tag{4}$$

$$(2U(i+1) - U(i+2))^2/2,$$

again, depending on the direction of the flow information. In this way, the dependent variable extrapolation technique yields

$$2U(i)^2 - 2U(i)U(i-1) + U(i-1)^2/2 \quad \text{or} \tag{5}$$

$$2U(i+1)^2 - 2U(i+1)U(i+2) + U(i+2)^2/2\ .$$

This result shows an extra term, $-2U(i+1)U(i+2)$, (as compared to Equation 3) which will have some effects that are inherent to this type of numerical method.

2. DIFFERENCING TECHNIQUES

The flow solvers (Euler codes), being examined by our research, use two types of differencing techniques to solve for the flux at the face of a cell; both of these techniques have been developed by Whitfield (References 4, 5, and 6).

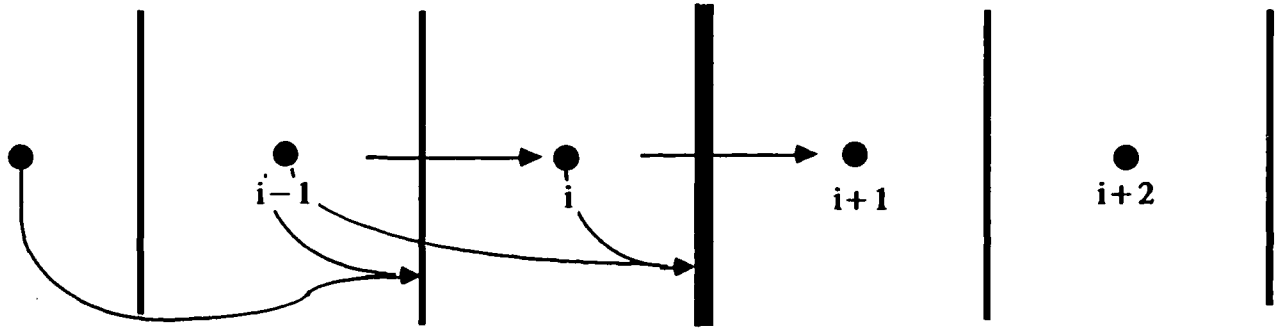

Figure 1. Finite-Volume, Two-point Extrapolation Technique

The first differencing technique (Figure 2) employs a dependent variable averaging (DVA) approach to determine the direction of the flow of information across a cell face. For a specific cell face, the value of the dependent variable (U) is averaged from both sides of the cell. This yields a value for the dependent variable and, depending on the sign of U, is used to extrapolate (using one of the techniques discussed above) from one side of the cell face or the other, to obtain a value for the flux at the face of the cell.

The second differencing technique (Figure 3) employs a dual dependent variable technique (DDV) in which the value for the dependent variable (U) is determined for both sides of the cell face and, depending on the sign of U, can utilize both values of the dependent variable if the direction of the flow of information is toward the cell face from both directions. The direction of the flow of information determines whether the value of the dependent variable, U, is used from one side of the cell face (or the other) or from both sides, to extrapolate the flux to the cell face.

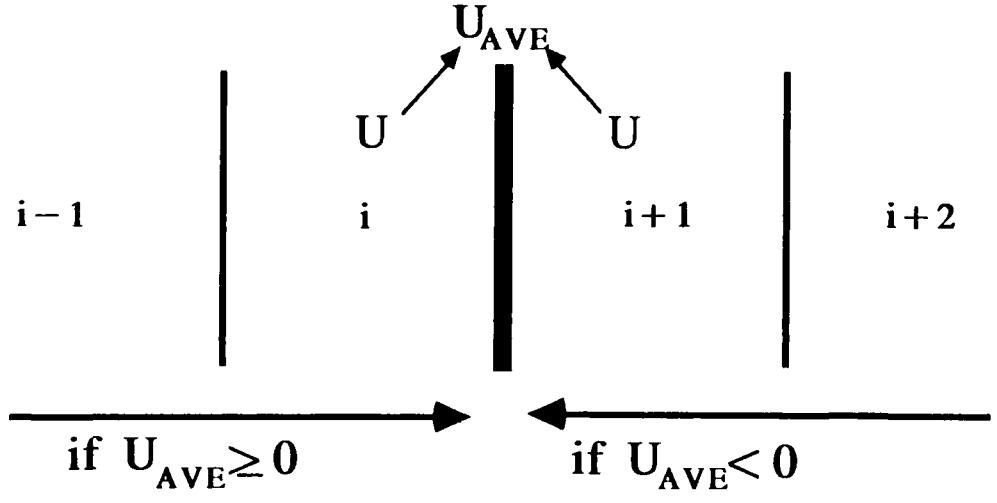

Figure 2. Dependent Variable Average (DVA) Difference Technique

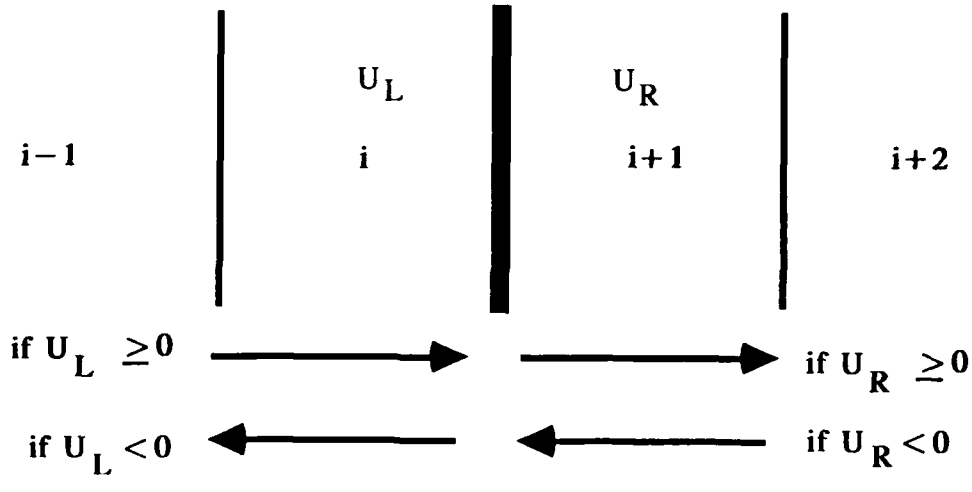

Figure 3. Dual Dependent Variable (DDV) Difference Technique

SECTION IV

NUMERICAL RESULTS

For this analysis, both the extrapolation and differencing techniques are examined using the inviscid Burgers equation to model the propagation of a wave in time. The numerical analysis used here to study the inviscid Burgers equation should yield second-order accurate results. This level of accuracy is typified by dispersion or ringing effects which overshoot the actual, physical results.

The first phase of our study looks at forcing a wave to propagate in only one direction. This allows us to better examine the differences between the two extrapolation techniques; since the wave is moving in only one direction, the differencing techniques are essentially the same. Figure 4a shows the effects of using the DVA technique with dependent variable extrapolation. The results are atypical, for a second-order accurate solution method, in that no dispersive effects (ringing) are apparent downwind of the wave. Figure 4b gives the results for the DVA technique using flux extrapolation. These results show the characteristic dispersive effects yielded by a second-order scheme in which the numerical solution overshoots the exact solution on the downwind side of the shock. Figure 4c shows results for the DDV technique with dependent variable extrapolation in which we again observe what appears to be dissipative characteristics to a second-order scheme. In Figure 4d the results are given for the DDV technique using flux extrapolation. Once again the flux extrapolation approach yields typical second-order results with ringing effects. To better study the effects of the extrapolation approaches, a Courant number of 1.50 was used since at a Courant number of either 1.00 or 2.00 the numerical technique yields the exact solution (by satisfying the shift condition in Equation B.9) (Reference 1).

The second phase of our examination studies the effects of the two differencing approaches (DDV and DVA) by forcing two waves to meet at a cell face of equal velocities (magnitudes). A Courant number of 2.00 is employed so that the effects of the two extrapolation techniques are negated (by satisfying the shift condition in Equation B.9) (Reference). Figure 5a shows the results for the DVA technique using dependent variable extrapolation which yields the exact solution to the mathematical model. Similar results were yielded in Figure 5b for the DVA technique using flux extrapolation. Figure 5c yields the results for the DDV technique with dependent variable extrapolation and shows the exact solution, as does Figure 5d for the DDV technique using flux extrapolation. For this simple model both differencing techniques (DDV and DVA) yield the same results; therefore, a more complicated test must be accomplished to better understand the limitations of the approaches.

For the final phase of this investigation, all aspects of the problem are examined by forcing two waves to approach each other at unequal velocities (magnitudes). Due to the unequal velocities, U , the effective Courant number changes for each direction. Figure 6a shows the effects for the

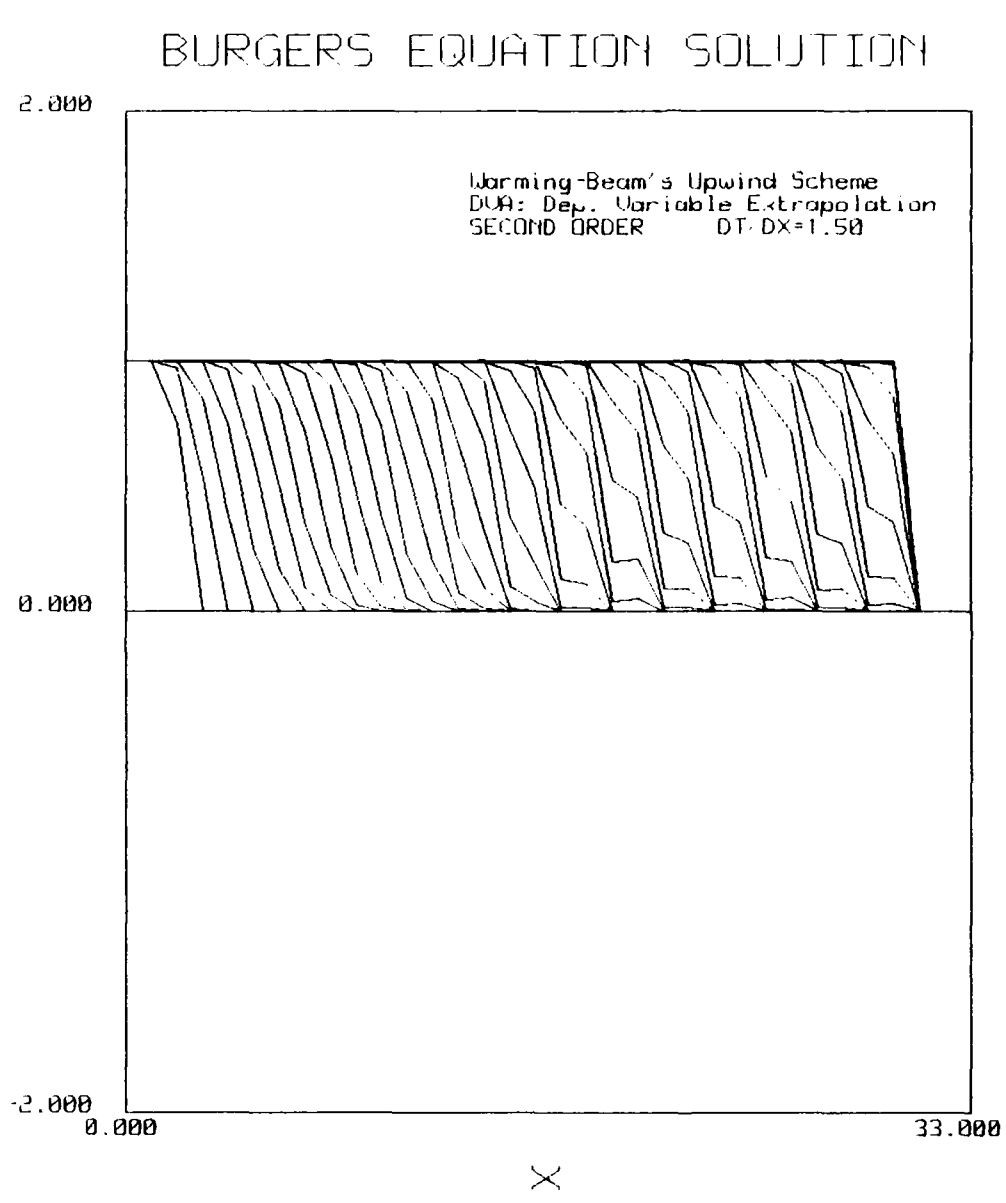

TIME STEP: 50

U(1)=	1.000000
U(2)=	1.000000
U(3)=	1.000000
U(4)=	1.000000
U(5)=	1.000000
U(6)=	1.000000
U(7)=	1.000000
U(8)=	1.000000
U(9)=	1.000000
U(10)=	1.000000
U(11)=	1.000000
U(12)=	1.000000
U(13)=	1.000000
U(14)=	1.000000
U(15)=	1.000000
U(16)=	1.000000
U(17)=	1.000000
U(18)=	1.000000
U(19)=	1.000000
U(20)=	1.000000
U(21)=	1.000000
U(22)=	1.000000
U(23)=	1.000000
U(24)=	1.000000
U(25)=	1.000000
U(26)=	1.000000
U(27)=	1.000000
U(28)=	1.000000
U(29)=	1.000000
U(30)=	1.000000
U(31)=	1.000000
U(32)=	0.0000000
U(33)=	0.0000000

Figure 4a. Burgers Equation Solution ν =1.50

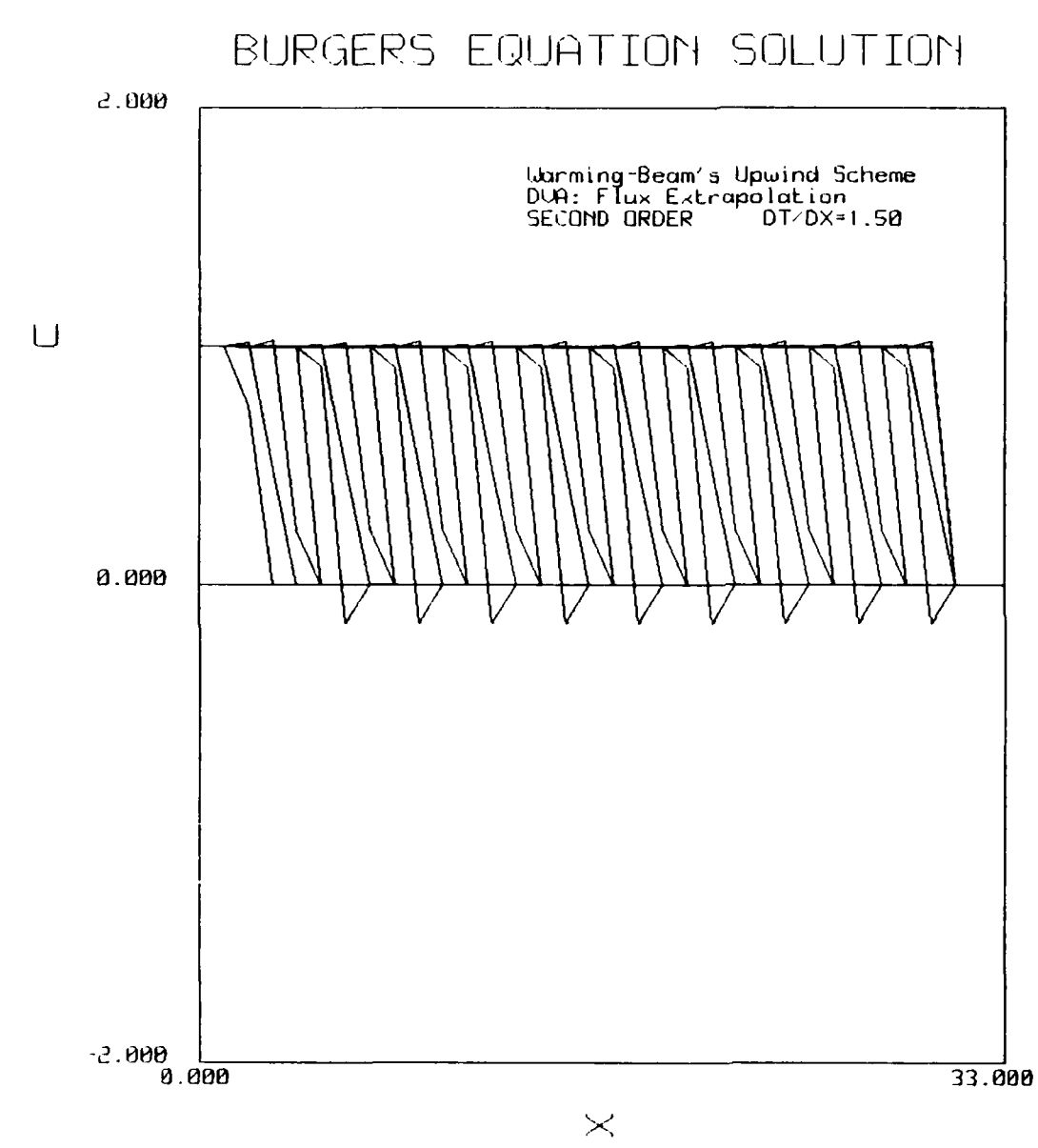

TIME STEP: 50

U(1)=	1.000000
U(2)=	1.000000
U(3)=	1.000000
U(4)=	1.000000
U(5)=	1.000000
U(6)=	1.000000
U(7)=	1.000000
U(8)=	1.000000
U(9)=	1.000000
U(10)=	1.000000
U(11)=	1.000000
U(12)=	1.000000
U(13)=	1.000000
U(14)=	1.000000
U(15)=	1.000000
U(16)=	1.000000
U(17)=	1.000000
U(18)=	1.000000
U(19)=	1.000000
U(20)=	1.000000
U(21)=	1.000000
U(22)=	1.000000
U(23)=	1.000000
U(24)=	1.000000
U(25)=	1.000000
U(26)=	1.000000
U(27)=	1.000000
U(28)=	1.000000
U(29)=	1.000000
U(30)=	1.000000
U(31)=	1.000000
U(32)=	0.0000000
U(33)=	0.0000000

Figure 4b. Burgers Equation Solution - $\nu = 1.50$

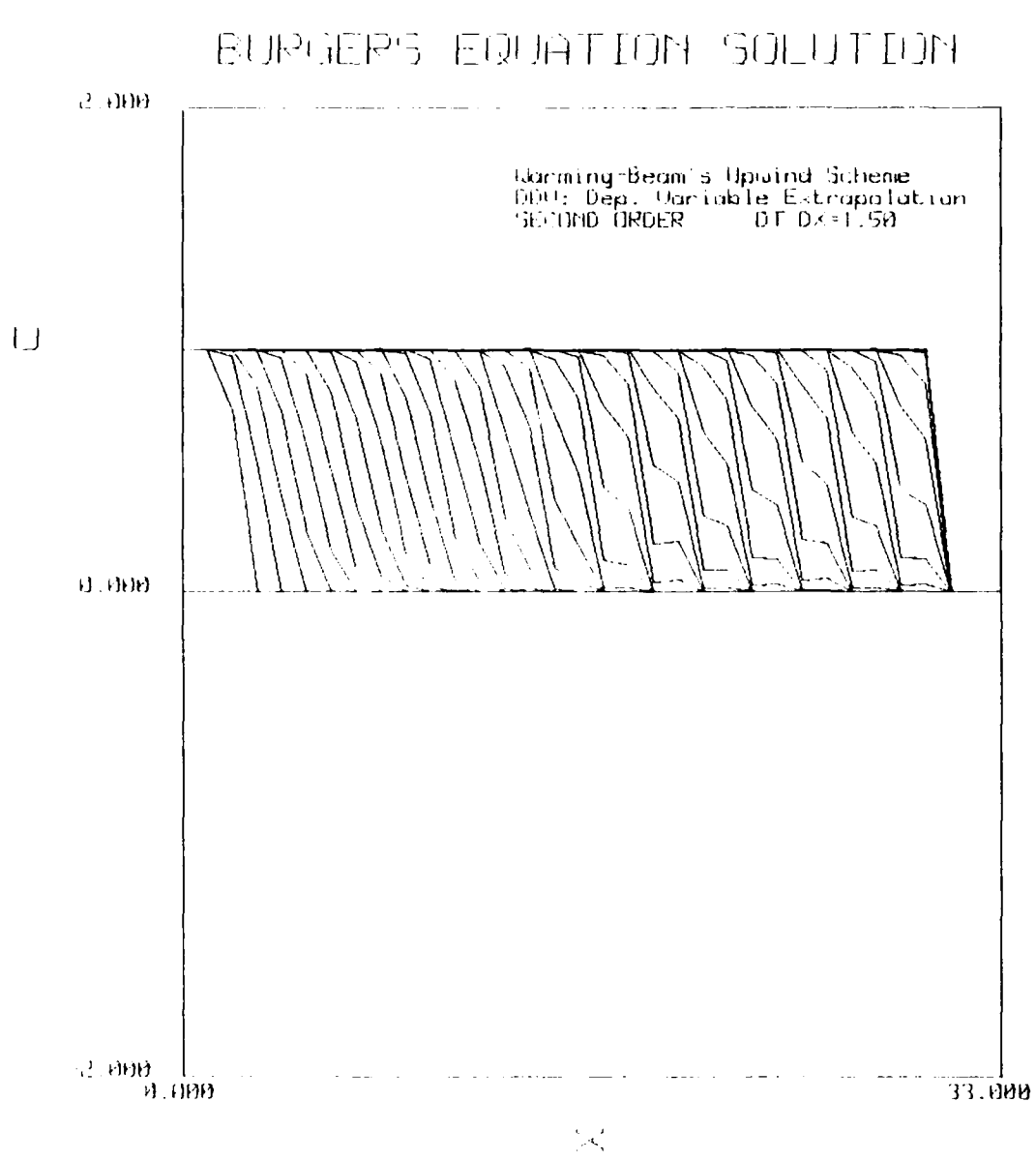

TIME STEP: 50

U(1)=	1.000000
U(2)=	1.000000
U(3)=	1.000000
U(4)=	1.000000
U(5)=	1.000000
U(6)=	1.000000
U(7)=	1.000000
U(8)=	1.000000
U(9)=	1.000000
U(10)=	1.000000
U(11)=	1.000000
U(12)=	1.000000
U(13)=	1.000000
U(14)=	1.000000
U(15)=	1.000000
U(16)=	1.000000
U(17)=	1.000000
U(18)=	1.000000
U(19)=	1.000000
U(20)=	1.000000
U(21)=	1.000000
U(22)=	1.000000
U(23)=	1.000000
U(24)=	1.000000
U(25)=	1.000000
U(26)=	1.000000
U(27)=	1.000000
U(28)=	1.000000
U(29)=	1.000000
U(30)=	1.000000
U(31)=	1.000000
U(32)=	0.0000000
U(33)=	0.0000000

Figure 4c. Burgers Equation Solution - $\nu = 1.50$

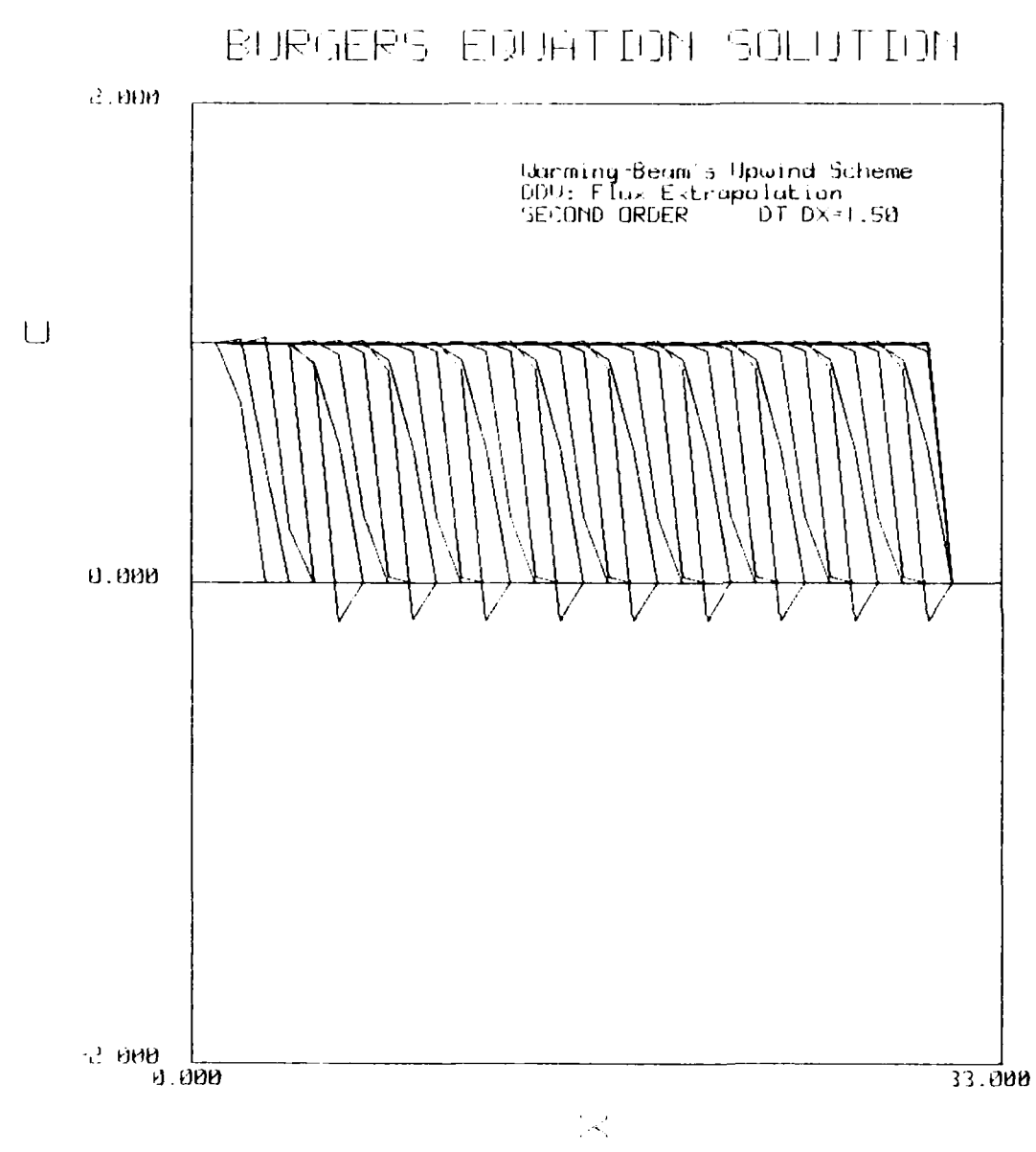

TIME STEP: 50

U(1)=	1.000000
U(2)=	1.000000
U(3)=	1.000000
U(4)=	1.000000
U(5)=	1.000000
U(6)=	1.000000
U(7)=	1.000000
U(8)=	1.000000
U(9)=	1.000000
U(10)=	1.000000
U(11)=	1.000000
U(12)=	1.000000
U(13)=	1.000000
U(14)=	1.000000
U(15)=	1.000000
U(16)=	1.000000
U(17)=	1.000000
U(18)=	1.000000
U(19)=	1.000000
U(20)=	1.000000
U(21)=	1.000000
U(22)=	1.000000
U(23)=	1.000000
U(24)=	1.000000
U(25)=	1.000000
U(26)=	1.000000
U(27)=	1.000000
U(28)=	1.000000
U(29)=	1.000000
U(30)=	1.000000
U(31)=	1.000000
U(32)=	0.0000000
U(33)=	0.0000000

Figure 4d. Burgers Equation Solution - $\nu = 1.50$

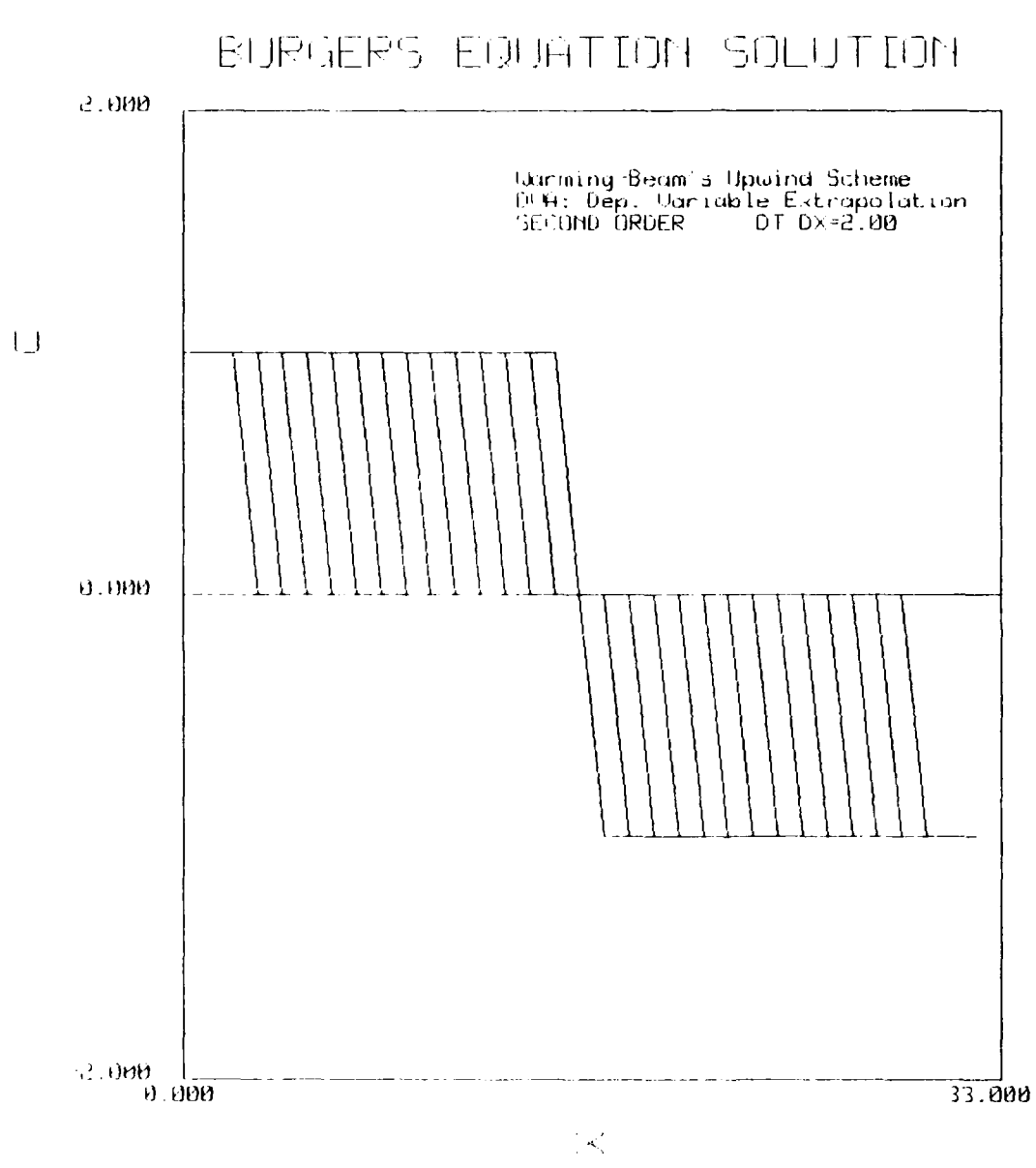

TIME STEP: 50

U(1)=	1.000000
U(2)=	1.000000
U(3)=	1.000000
U(4)=	1.000000
U(5)=	1.000000
U(6)=	1.000000
U(7)=	1.000000
U(8)=	1.000000
U(9)=	1.000000
U(10)=	1.000000
U(11)=	1.000000
U(12)=	1.000000
U(13)=	1.000000
U(14)=	1.000000
U(15)=	1.000000
U(16)=	1.000000
U(17)=	0.0000000
U(18)=	-1.000000
U(19)=	-1.000000
U(20)=	-1.000000
U(21)=	-1.000000
U(22)=	-1.000000
U(23)=	-1.000000
U(24)=	-1.000000
U(25)=	-1.000000
U(26)=	-1.000000
U(27)=	-1.000000
U(28)=	-1.000000
U(29)=	-1.000000
U(30)=	-1.000000
U(31)=	-1.000000
U(32)=	-1.000000
U(33)=	-1.000000

Figure 5a. Burgers Equation Solution - ν=2.00

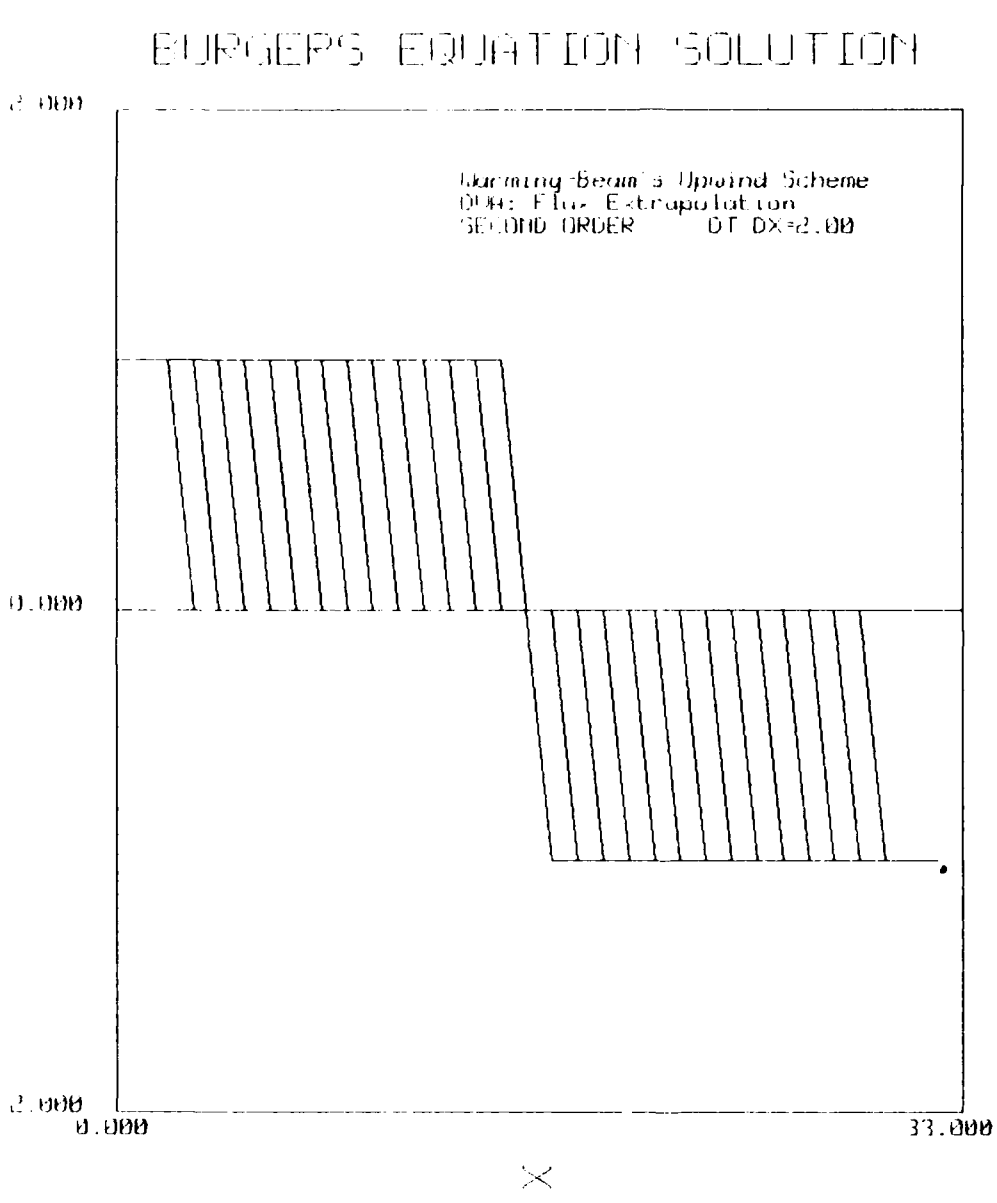

TIME STEP: 50

U(1)=	1.000000
U(2)=	1.000000
U(3)=	1.000000
U(4)=	1.000000
U(5)=	1.000000
U(6)=	1.000000
U(7)=	1.000000
U(8)=	1.000000
U(9)=	1.000000
U(10)=	1.000000
U(11)=	1.000000
U(12)=	1.000000
U(13)=	1.000000
U(14)=	1.000000
U(15)=	1.000000
U(16)=	1.000000
U(17)=	0.0000000
U(18)=	-1.000000
U(19)=	-1.000000
U(20)=	-1.000000
U(21)=	-1.000000
U(22)=	-1.000000
U(23)=	-1.000000
U(24)=	-1.000000
U(25)=	-1.000000
U(26)=	-1.000000
U(27)=	-1.000000
U(28)=	-1.000000
U(29)=	-1.000000
U(30)=	-1.000000
U(31)=	-1.000000
U(32)=	-1.000000
U(33)=	-1.000000

Figure 5b. Burgers Equation Solution - ν=2.00

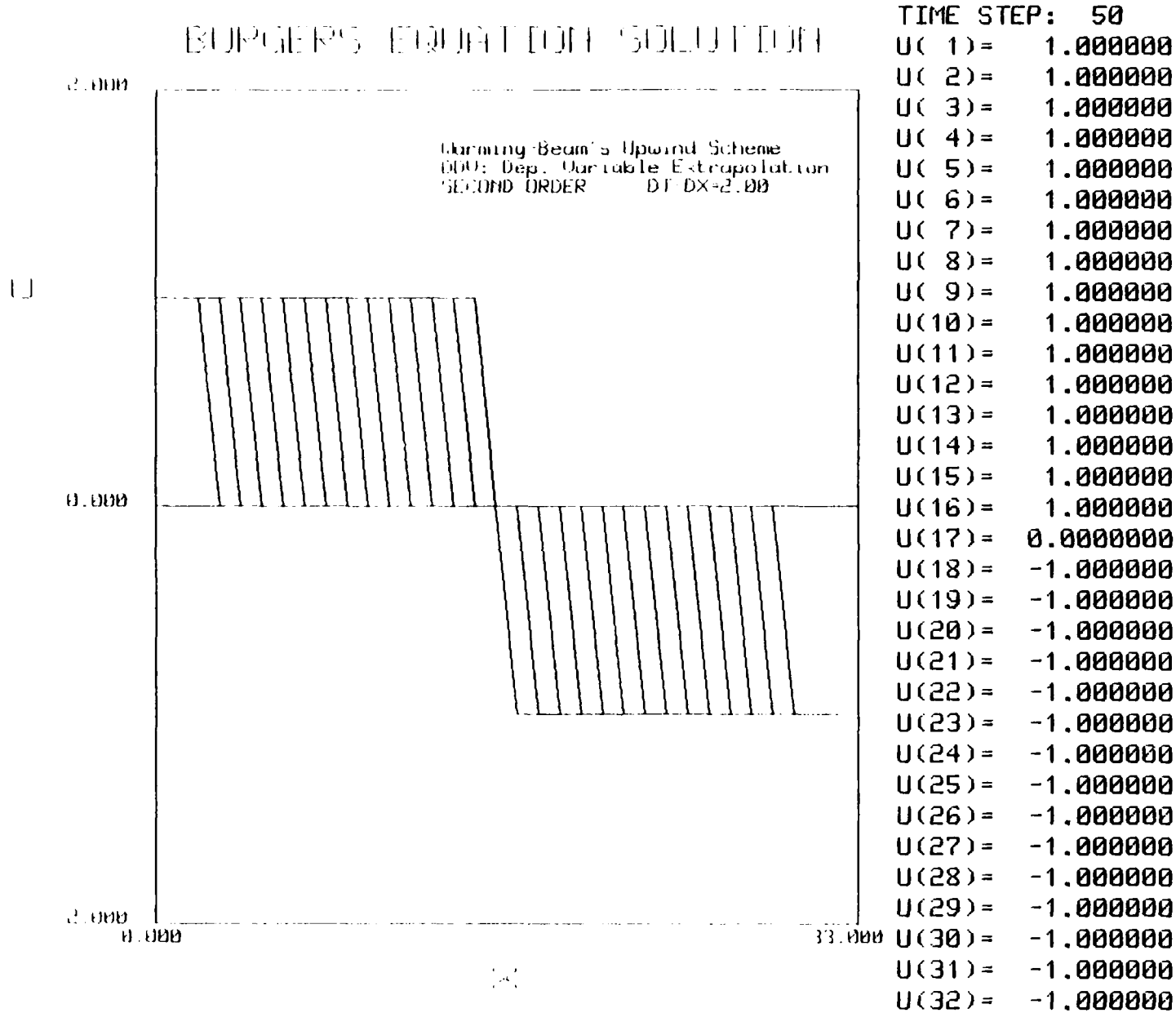

TIME STEP: 50

U(1)=	1.000000
U(2)=	1.000000
U(3)=	1.000000
U(4)=	1.000000
U(5)=	1.000000
U(6)=	1.000000
U(7)=	1.000000
U(8)=	1.000000
U(9)=	1.000000
U(10)=	1.000000
U(11)=	1.000000
U(12)=	1.000000
U(13)=	1.000000
U(14)=	1.000000
U(15)=	1.000000
U(16)=	1.000000
U(17)=	0.0000000
U(18)=	-1.000000
U(19)=	-1.000000
U(20)=	-1.000000
U(21)=	-1.000000
U(22)=	-1.000000
U(23)=	-1.000000
U(24)=	-1.000000
U(25)=	-1.000000
U(26)=	-1.000000
U(27)=	-1.000000
U(28)=	-1.000000
U(29)=	-1.000000
U(30)=	-1.000000
U(31)=	-1.000000
U(32)=	-1.000000
U(33)=	-1.000000

Figure 5c. Burgers Equation Solution - ν=2.00

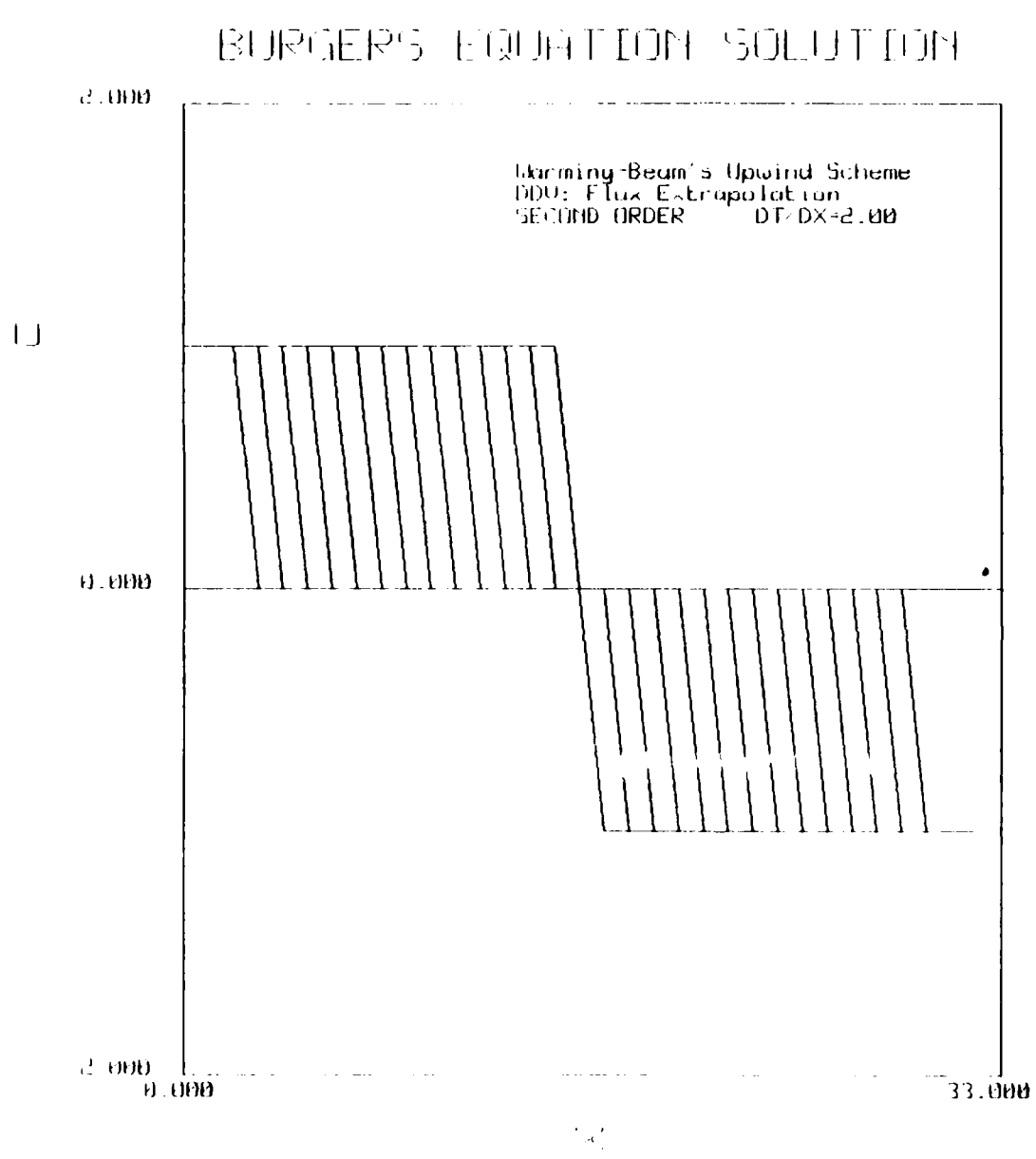

TIME STEP: 50

U(1)=	1.000000
U(2)=	1.000000
U(3)=	1.000000
U(4)=	1.000000
U(5)=	1.000000
U(6)=	1.000000
U(7)=	1.000000
U(8)=	1.000000
U(9)=	1.000000
U(10)=	1.000000
U(11)=	1.000000
U(12)=	1.000000
U(13)=	1.000000
U(14)=	1.000000
U(15)=	1.000000
U(16)=	1.000000
U(17)=	0.0000000
U(18)=	-1.000000
U(19)=	-1.000000
U(20)=	-1.000000
U(21)=	-1.000000
U(22)=	-1.000000
U(23)=	-1.000000
U(24)=	-1.000000
U(25)=	-1.000000
U(26)=	-1.000000
U(27)=	-1.000000
U(28)=	-1.000000
U(29)=	-1.000000
U(30)=	-1.000000
U(31)=	-1.000000
U(32)=	-1.000000
U(33)=	-1.000000

Figure 5d. Burgers Equation Solution - ν= 2.00

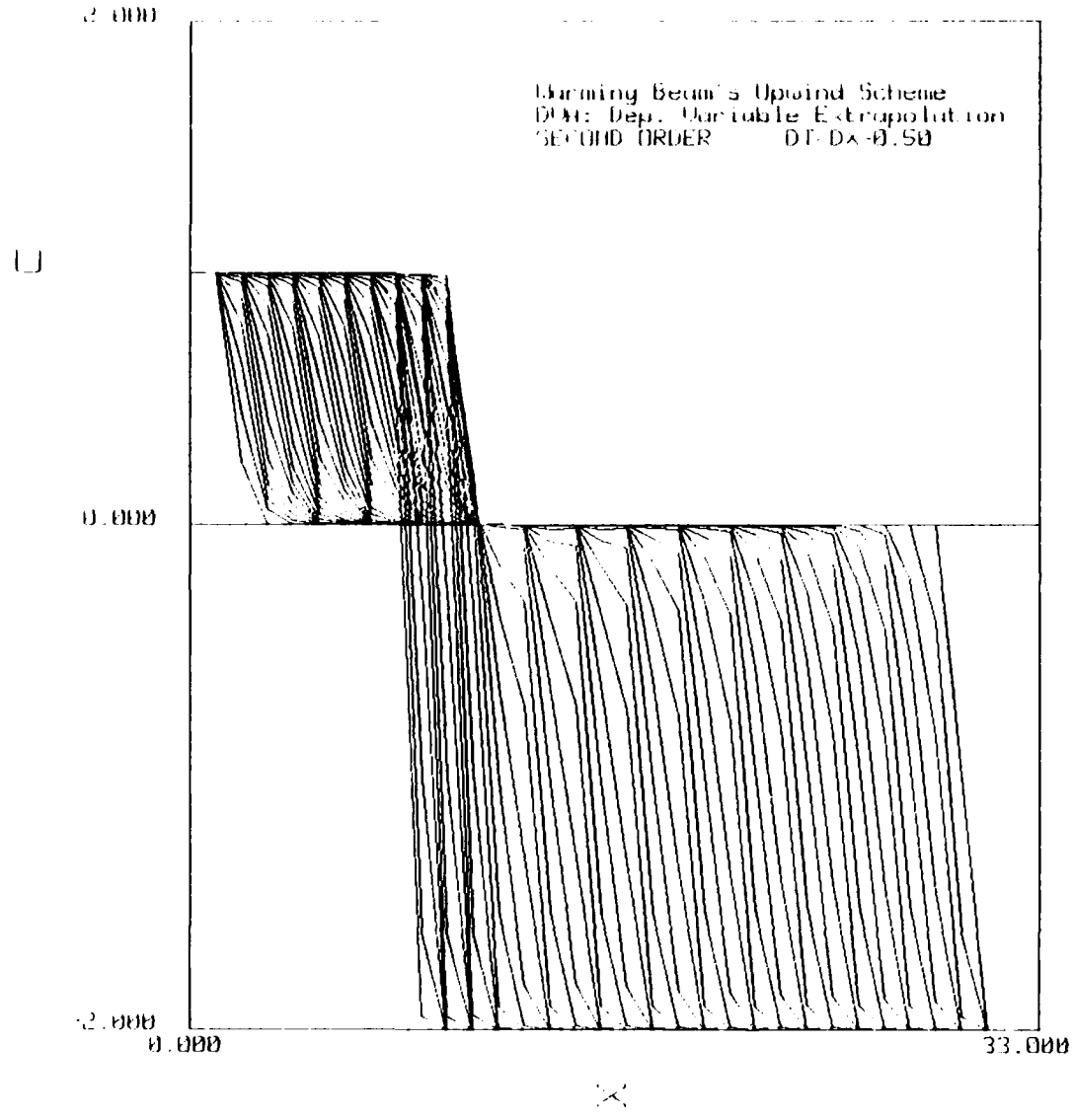

TIME STEP: 50

U(1)=	1.000000
U(2)=	1.000000
U(3)=	1.000000
U(4)=	1.000000
U(5)=	1.000000
U(6)=	1.000000
U(7)=	1.000000
U(8)=	1.000000
U(9)=	0.4448777
U(10)=	-1.944878
U(11)=	-2.000000
U(12)=	-2.000000
U(13)=	-2.000000
U(14)=	-2.000000
U(15)=	-2.000000
U(16)=	-2.000000
U(17)=	-2.000000
U(18)=	-2.000000
U(19)=	-2.000000
U(20)=	-2.000000
U(21)=	-2.000000
U(22)=	-2.000000
U(23)=	-2.000000
U(24)=	-2.000000
U(25)=	-2.000000
U(26)=	-2.000000
U(27)=	-2.000000
U(28)=	-2.000000
U(29)=	-2.000000
U(30)=	-2.000000
U(31)=	-2.000000
U(32)=	-2.000000
U(33)=	-2.000000

Figure 6a. Burgers Equation Solution

DDV technique with dependent variable extrapolation. The results show the atypical (dissipative) solution yielded by the dependent variable extrapolation. As the waves meet, the wave with the greater magnitude runs over the lesser wave at an average wave speed. In Figure 6b we obtain the results for the DVA technique using flux extrapolation. This approach yields the expected second-order results and also shows the greater magnitude wave running over the lesser wave at an average (or deduced) velocity. Figure 6c shows results, similar to those in Figure 6a, for the DDV techniques using the dependent variable extrapolation approach. As in Figure 6a, we observe the dissipative effects on the solution and the propagation of the larger wave at an average speed after the collision. Figure 6d shows the results for the DDV technique with flux extrapolation. As in Figure 6b, the expected dispersive effects are observed and, again, the greater wave moves at an average velocity after the collision.

A further analysis was performed to attempt to find weaknesses in the different approaches. In this case the effective Courant number was doubled thereby pushing the CFL condition towards its limit of 2.00. Figure 6e shows results, similar to those in Figure 6a, for the DVA technique with dependent variable extrapolation; however, the propagation of the wave after the collision has twice the velocity. In Figure 6f the results are, again, similar to those in Figure 6b with the exception of the wave propogation being at twice the speed. Figure 6g shows the only major discrepancy in our analysis. The DDV technique with dependent variable extrapolation shows good results until the meeting point for the unequal waves. At the collision due to diffusive effects, the effective Courant number goes well above the stability limit of 2.00 and the solution diverges. However, when the DDV technique is applied with flux extrapolation (Figure 6h), we again obtain typical results similar to those in Figure 6d.

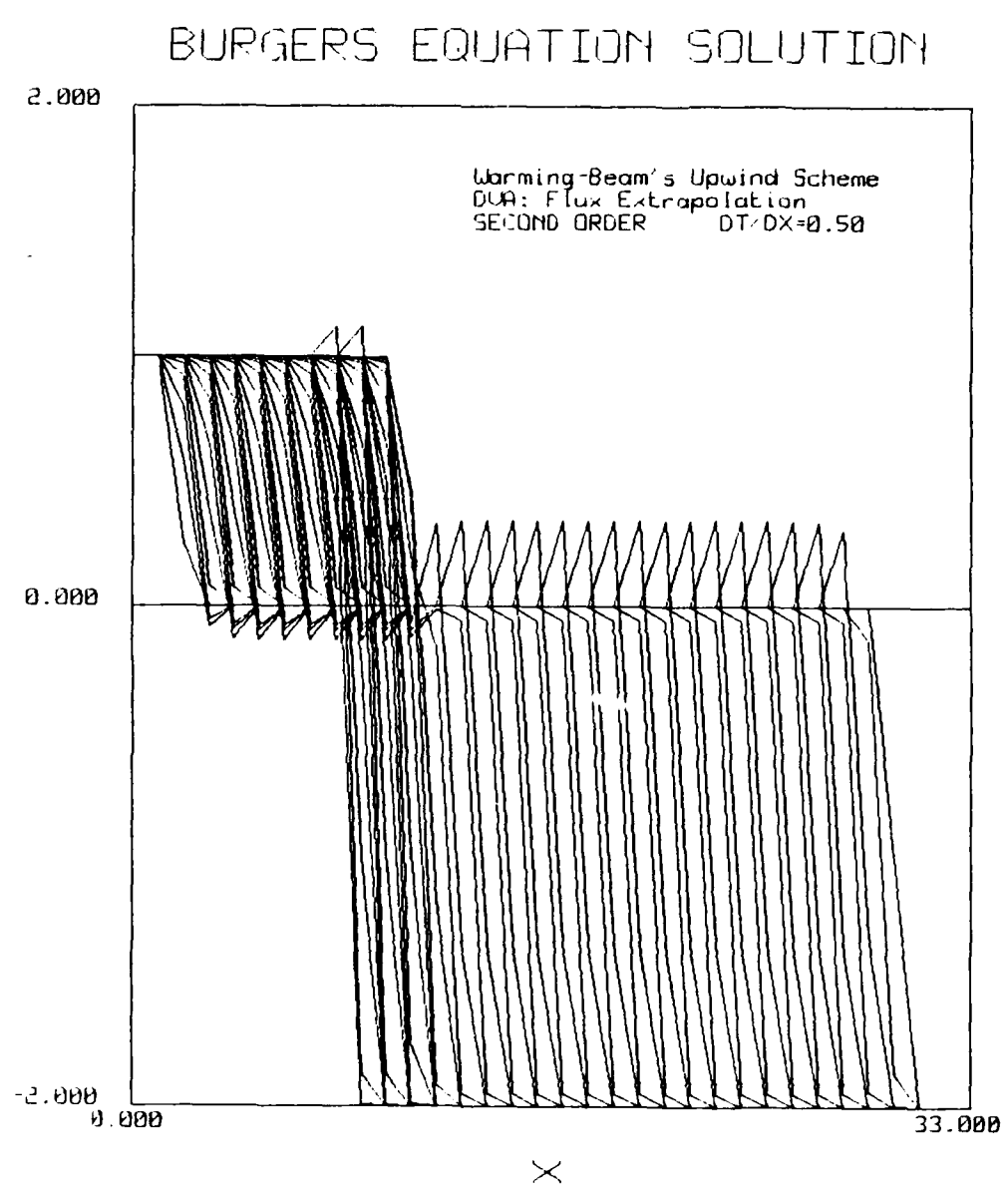

TIME STEP: 50

U(1)=	1.000000
U(2)=	1.000000
U(3)=	1.000000
U(4)=	1.000000
U(5)=	1.000000
U(6)=	1.000000
U(7)=	1.000000
U(8)=	1.000000
U(9)=	0.4977927
U(10)=	-1.997793
U(11)=	-2.000000
U(12)=	-2.000000
U(13)=	-2.000000
U(14)=	-2.000000
U(15)=	-2.000000
U(16)=	-2.000000
U(17)=	-2.000000
U(18)=	-2.000000
U(19)=	-2.000000
U(20)=	-2.000000
U(21)=	-2.000000
U(22)=	-2.000000
U(23)=	-2.000000
U(24)=	-2.000000
U(25)=	-2.000000
U(26)=	-2.000000
U(27)=	-2.000000
U(28)=	-2.000000
U(29)=	-2.000000
U(30)=	-2.000000
U(31)=	-2.000000
U(32)=	-2.000000
U(33)=	-2.000000

Figure 6b. Burgers Equation Solution

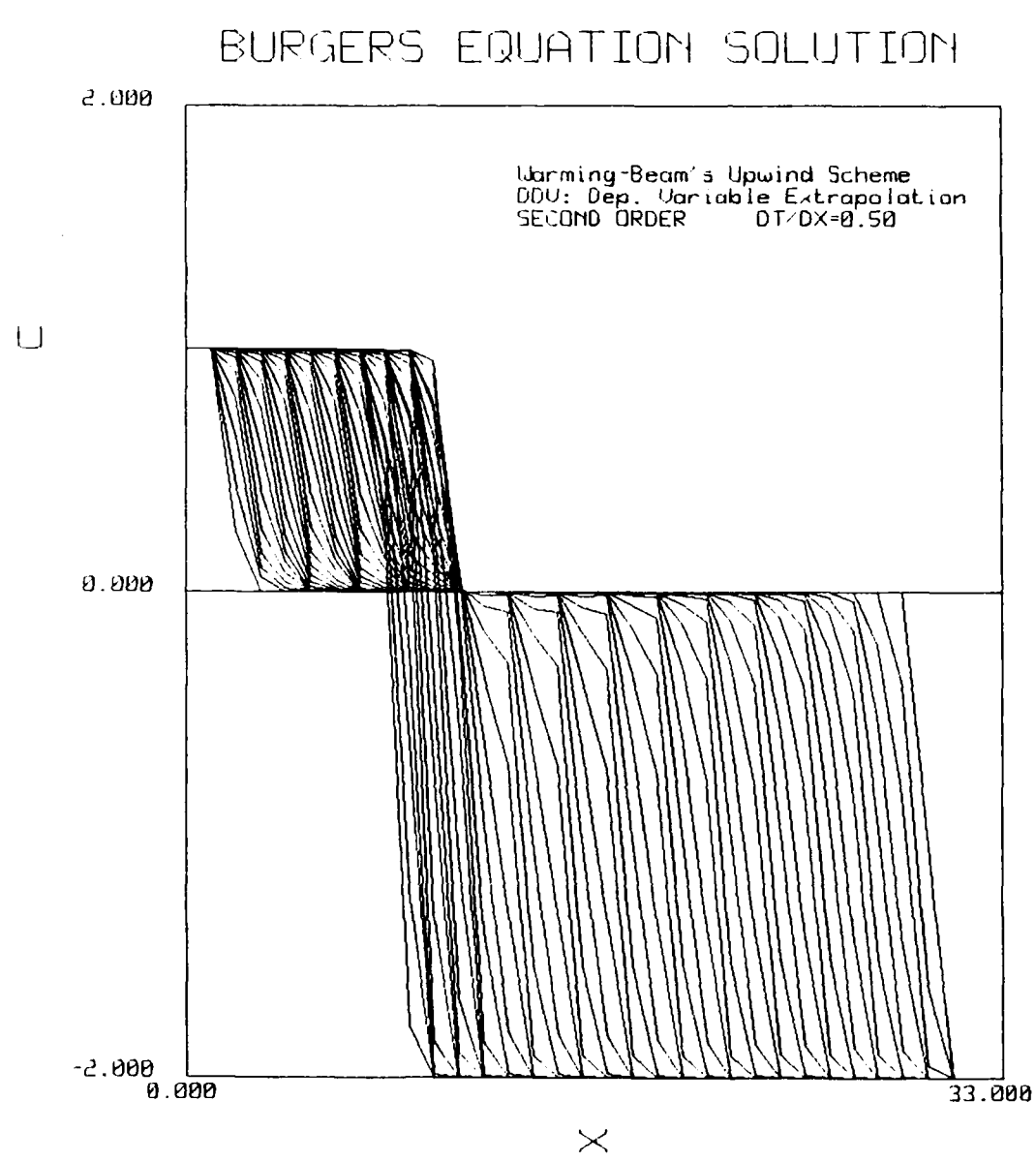


```
TIME STEP:  50
U( 1)=   1.000000
U( 2)=   1.000000
U( 3)=   1.000000
U( 4)=   1.000000
U( 5)=   1.000000
U( 6)=   1.000000
U( 7)=   1.000000
U( 8)=   1.000000
U( 9)=  0.2885044
U(10)=  -1.788504
U(11)=  -2.000000
U(12)=  -2.000000
U(13)=  -2.000000
U(14)=  -2.000000
U(15)=  -2.000000
U(16)=  -2.000000
U(17)=  -2.000000
U(18)=  -2.000000
U(19)=  -2.000000
U(20)=  -2.000000
U(21)=  -2.000000
U(22)=  -2.000000
U(23)=  -2.000000
U(24)=  -2.000000
U(25)=  -2.000000
U(26)=  -2.000000
U(27)=  -2.000000
U(28)=  -2.000000
U(29)=  -2.000000
U(30)=  -2.000000
U(31)=  -2.000000
U(32)=  -2.000000
U(33)=  -2.000000
```

Figure 6c. Burgers Equation Solution

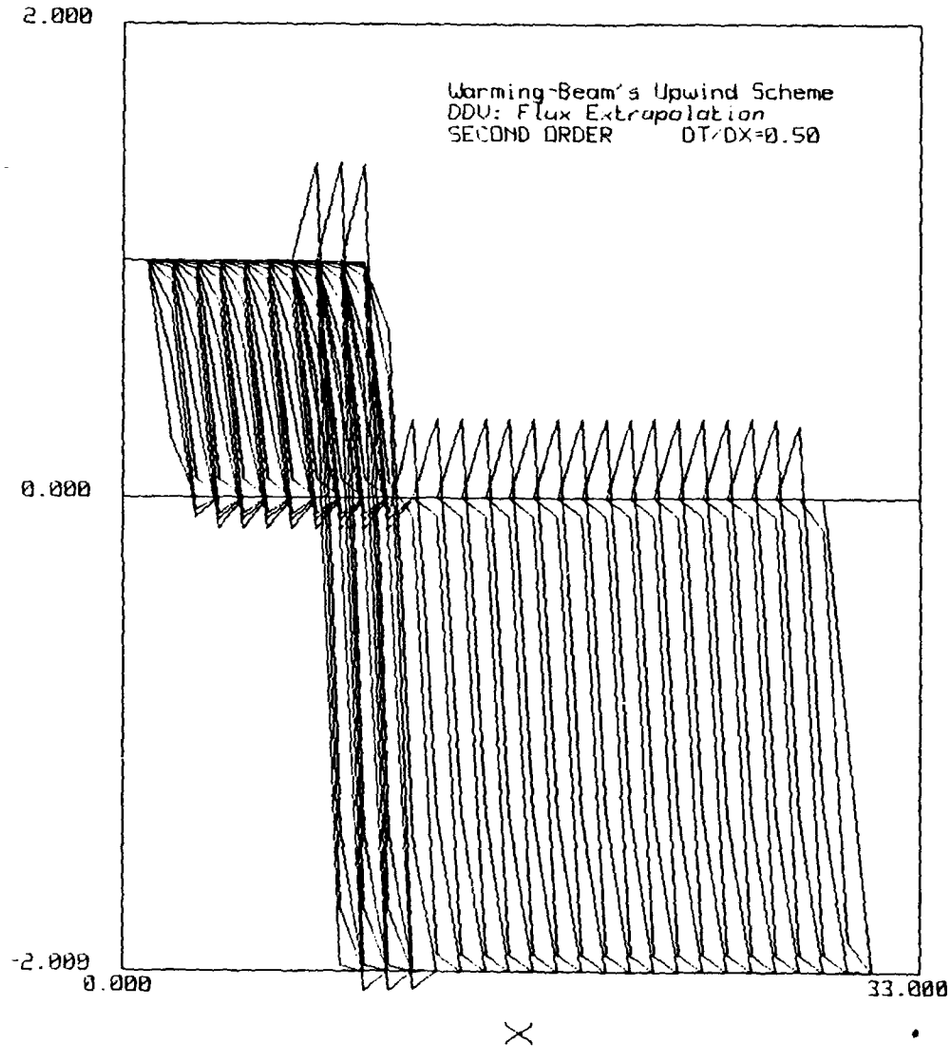

TIME STEP: 50

U(1)=	1.000000
U(2)=	1.000000
U(3)=	1.000000
U(4)=	1.000000
U(5)=	1.000000
U(6)=	1.000000
U(7)=	1.000000
U(8)=	1.000000
U(9)=	0.4795874
U(10)=	-1.979588
U(11)=	-2.000000
U(12)=	-2.000000
U(13)=	-2.000000
U(14)=	-2.000000
U(15)=	-2.000000
U(16)=	-2.000000
U(17)=	-2.000000
U(18)=	-2.000000
U(19)=	-2.000000
U(20)=	-2.000000
U(21)=	-2.000000
U(22)=	-2.000000
U(23)=	-2.000000
U(24)=	-2.000000
U(25)=	-2.000000
U(26)=	-2.000000
U(27)=	-2.000000
U(28)=	-2.000000
U(29)=	-2.000000
U(30)=	-2.000000
U(31)=	-2.000000
U(32)=	-2.000000
U(33)=	-2.000000

Figure 6d. Burgers Equation Solution

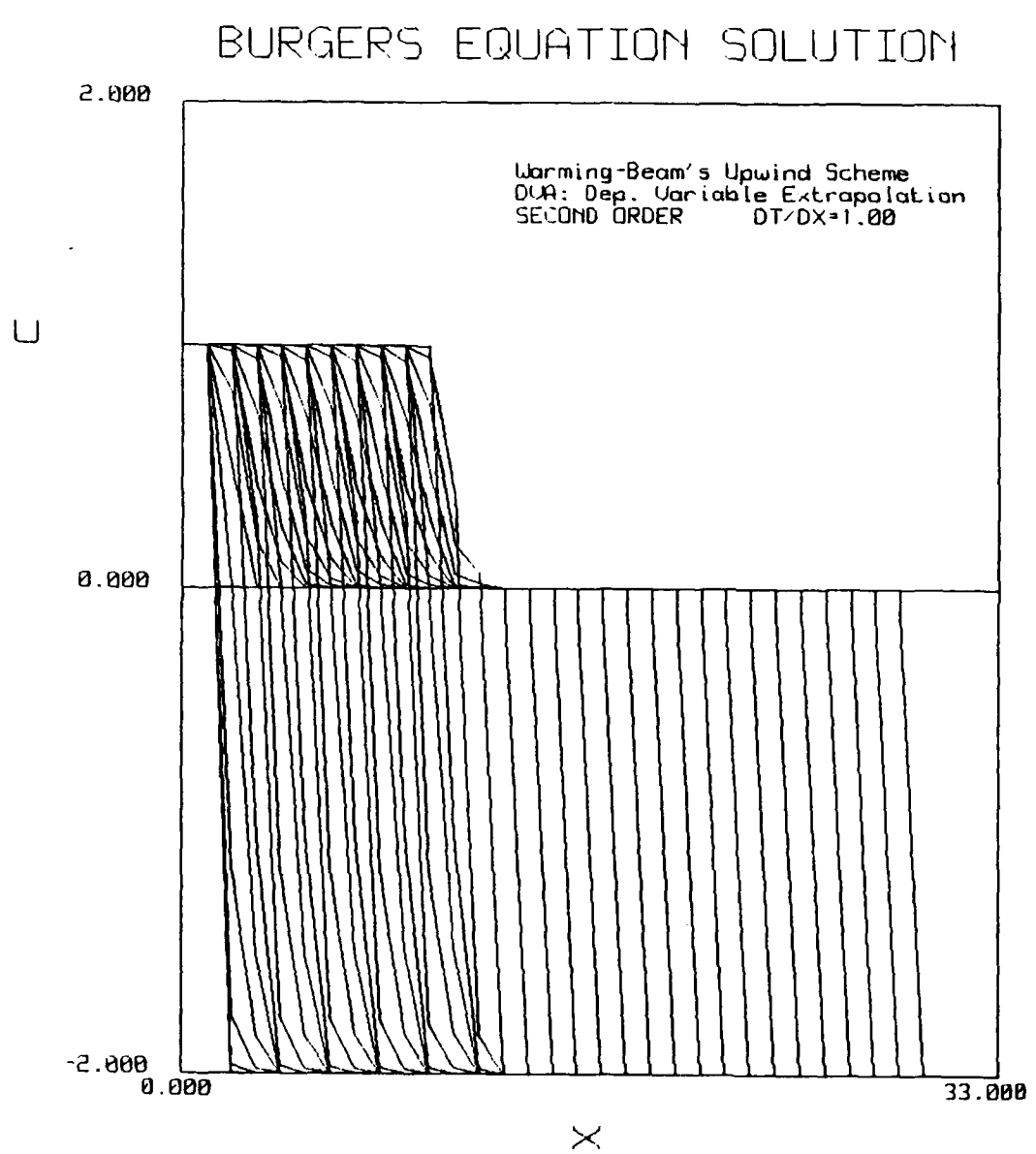

TIME STEP: 50

U(1)=	1.000000
U(2)=	1.000000
U(3)=	-2.000000
U(4)=	-2.000000
U(5)=	-2.000000
U(6)=	-2.000000
U(7)=	-2.000000
U(8)=	-2.000000
U(9)=	-2.000000
U(10)=	-2.000000
U(11)=	-2.000000
U(12)=	-2.000000
U(13)=	-2.000000
U(14)=	-2.000000
U(15)=	-2.000000
U(16)=	-2.000000
U(17)=	-2.000000
U(18)=	-2.000000
U(19)=	-2.000000
U(20)=	-2.000000
U(21)=	-2.000000
U(22)=	-2.000000
U(23)=	-2.000000
U(24)=	-2.000000
U(25)=	-2.000000
U(26)=	-2.000000
U(27)=	-2.000000
U(28)=	-2.000000
U(29)=	-2.000000
U(30)=	-2.000000
U(31)=	-2.000000
U(32)=	-2.000000
U(33)=	-2.000000

Figure 6e. Burgers Equation Solution

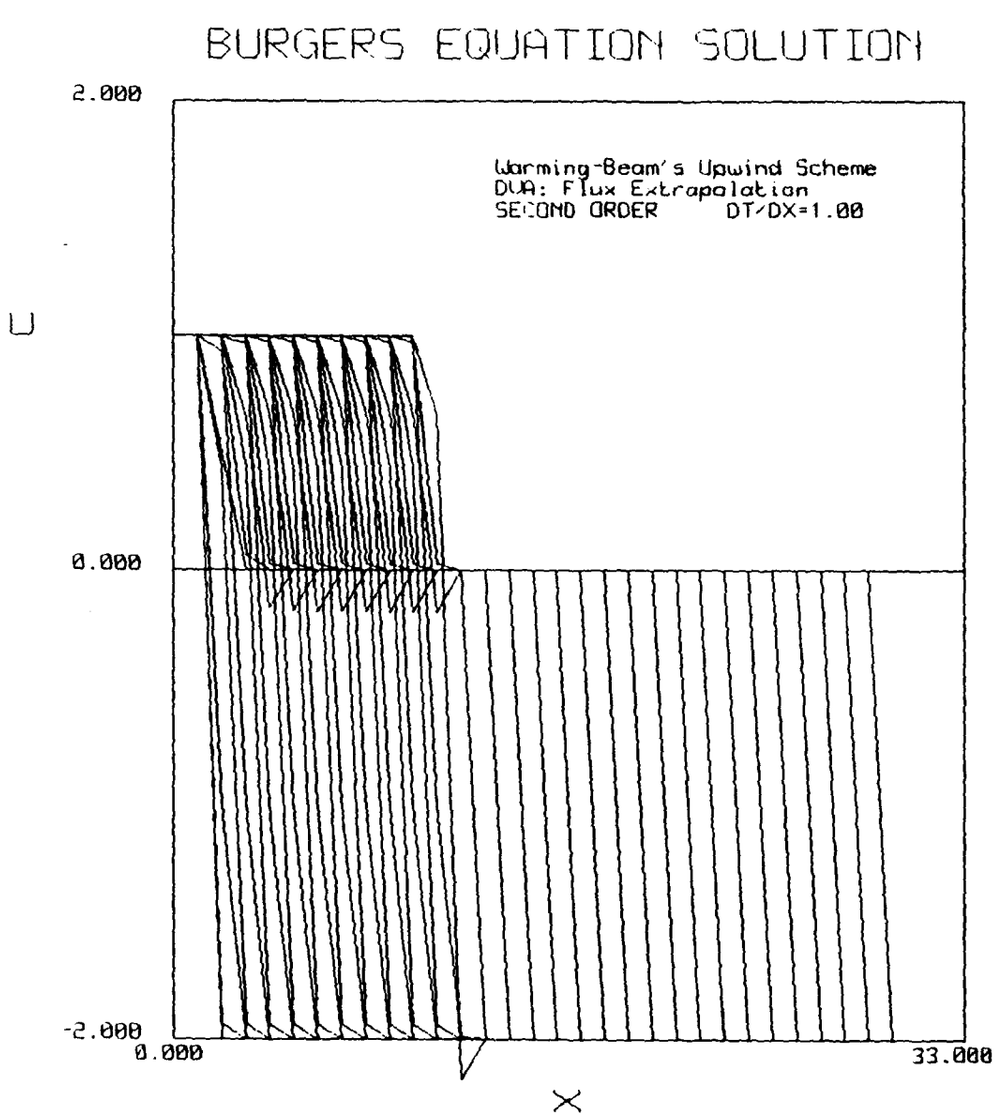

TIME STEP: 50

U(1)=	1.000000
U(2)=	1.000000
U(3)=	-2.000000
U(4)=	-2.000000
U(5)=	-2.000000
U(6)=	-2.000000
U(7)=	-2.000000
U(8)=	-2.000000
U(9)=	-2.000000
U(10)=	-2.000000
U(11)=	-2.000000
U(12)=	-2.000000
U(13)=	-2.000000
U(14)=	-2.000000
U(15)=	-2.000000
U(16)=	-2.000000
U(17)=	-2.000000
U(18)=	-2.000000
U(19)=	-2.000000
U(20)=	-2.000000
U(21)=	-2.000000
U(22)=	-2.000000
U(23)=	-2.000000
U(24)=	-2.000000
U(25)=	-2.000000
U(26)=	-2.000000
U(27)=	-2.000000
U(28)=	-2.000000
U(29)=	-2.000000
U(30)=	-2.000000
U(31)=	-2.000000
U(32)=	-2.000000
U(33)=	-2.000000

Figure 6f. Burgers Equation Solution

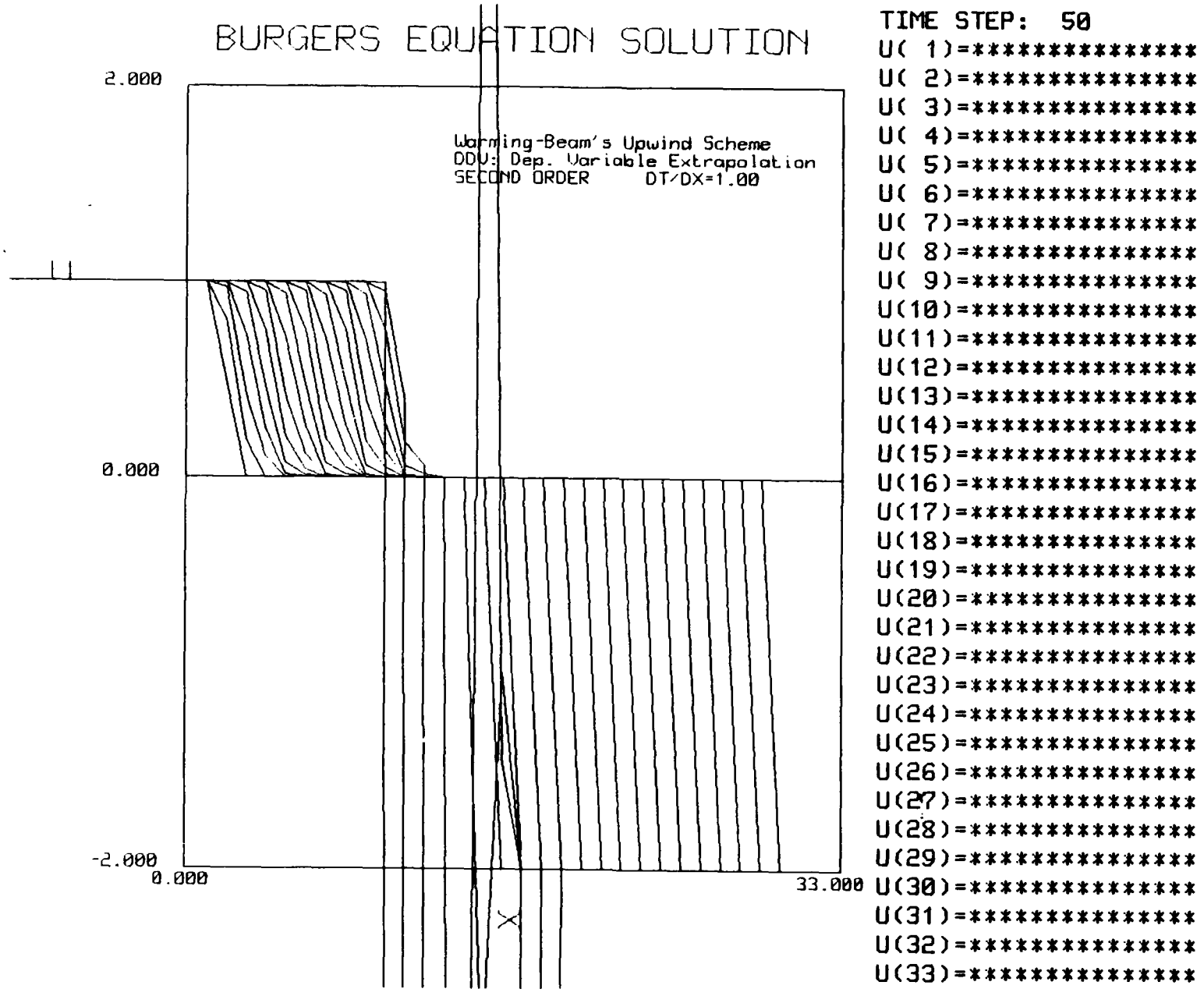

Figure 6g. Burgers Equation Solution

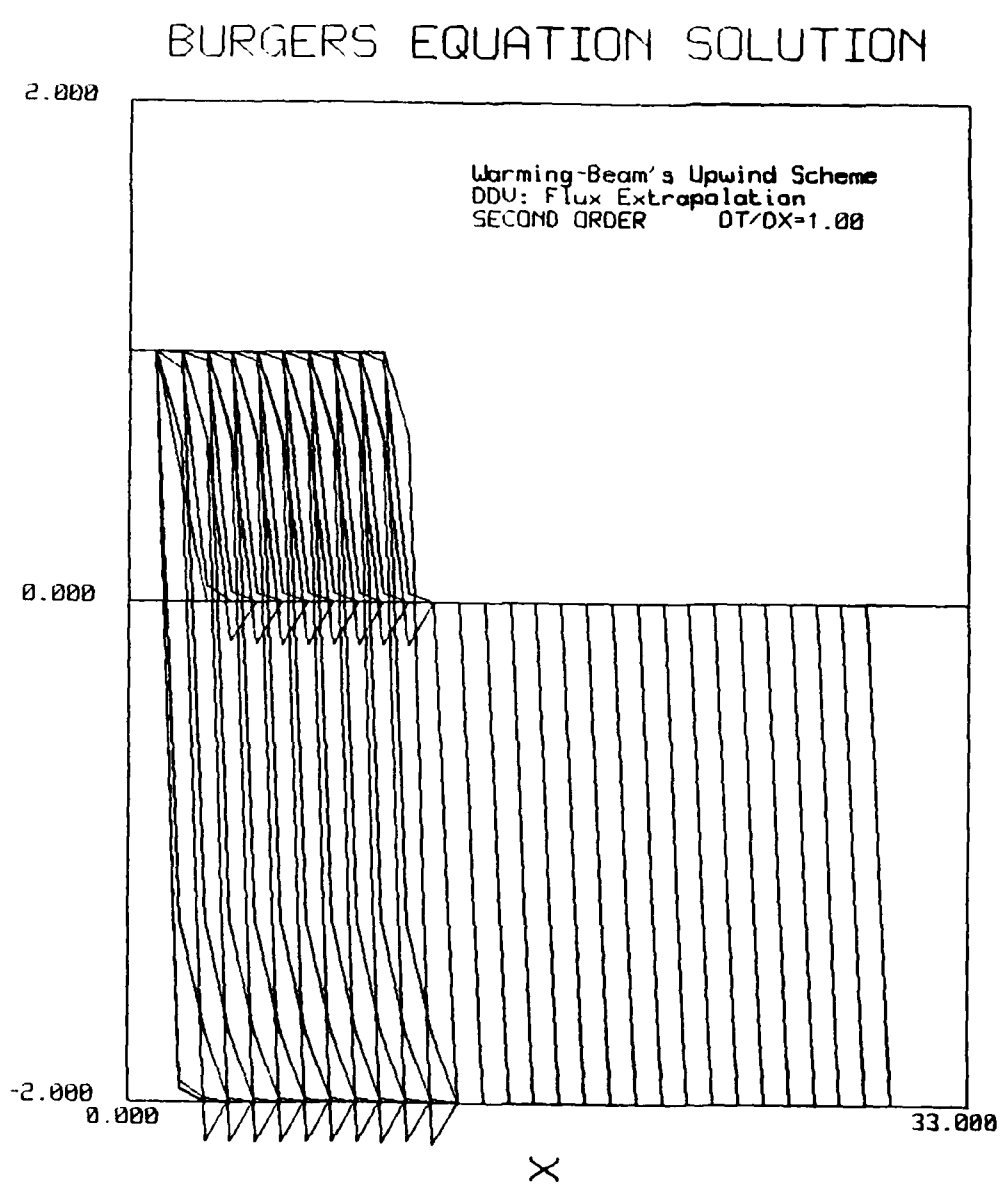

TIME STEP: 50

U(1)=	1.000000
U(2)=	1.000000
U(3)=	-1.949253
U(4)=	-2.000000
U(5)=	-2.000000
U(6)=	-2.000000
U(7)=	-2.000000
U(8)=	-2.000000
U(9)=	-2.000000
U(10)=	-2.000000
U(11)=	-2.000000
U(12)=	-2.000000
U(13)=	-2.000000
U(14)=	-2.000000
U(15)=	-2.000000
U(16)=	-2.000000
U(17)=	-2.000000
U(18)=	-2.000000
U(19)=	-2.000000
U(20)=	-2.000000
U(21)=	-2.000000
U(22)=	-2.000000
U(23)=	-2.000000
U(24)=	-2.000000
U(25)=	-2.000000
U(26)=	-2.000000
U(27)=	-2.000000
U(28)=	-2.000000
U(29)=	-2.000000
U(30)=	-2.000000
U(31)=	-2.000000
U(32)=	-2.000000
U(33)=	-2.000000

Figure 6h. Burgers Equation Solution

SECTION V

CONCLUSION

This investigation has yielded several important conclusions dealing with both the extrapolation techniques and the differencing approaches.

(1) The dependent variable extrapolation technique, used for both the dual dependent variable (DDV) and the dependent variable averaging (DVA) differencing methods, tends to negate the typical dispersive effects found in second-order accurate schemes. This is primarily due to the extra term found when applying the dependent variable extrapolation to the inviscid Burgers equation. When applying the flux extrapolation technique to both differencing methods, the expected dispersive effects are obtained.

(2) No significant differences were apparent when comparing the differencing techniques (dual dependent variable and dependent variable averaging). Both techniques closely modeled the correct mathematical solution, when using the flux extrapolation approach, throughout most of the investigation. The only inconsistency in the study occurred when the DDV differencing approach was used with dependent variable extrapolation (Figure 6g). In general, this tends to show that the DVA approach may be a more robust method than the DDV approach.

Therefore, the recommended approach to solving the inviscid Burgers equation for this examination is to apply the dependent variable averaging differencing technique with flux extrapolation. This method will also be directly applied to the three-dimensional Euler equations for the solution of the inviscid flow field about arbitrarily shaped weapon/store configurations.

APPENDIX A

INVISCID BURGERS EQUATION

Burgers equation (1948) can serve as a nonlinear analog of the fluid mechanics equations. This single equation has terms that closely duplicate the physical properties of the fluid equations, i.e., the model equation has a convective term, a diffusive or dissipative term, and a time-dependent term. (Reference 1)

$$\underset{\text{Unsteady term}}{U_t} + \underset{\text{Convective term}}{UU_x} = \underset{\text{Viscous term}}{U_{xx}} \qquad (A.1)$$

Equation (A.1) is parabolic when the viscous term is included and is a good model for the boundary-layer equations, the parabolized Navier-Stokes (PNS) equations and the complete Navier-Stokes equations. If the viscous term is neglected (inviscid Burgers equation), the remaining equation is composed of the unsteady term (U_t) and the nonlinear convection term (UU_x). The resulting hyperbolic equation

$$U_t + UU_x = 0; \qquad (A.2a)$$

in conservation law form

$$U_t + (U^2/2) = 0, \qquad (A.2b)$$

may be considered a simple analog of the Euler eqautions for the flow of an inviscid fluid. The analogy can be drawn due to the fact that both equations are first-order, hyperbolic, quasi-linear, partial differential equations and both model discontinuities, such as shocks, in the flow field (Reference 1).

Burger equation is a partial differential equation because U=U(x,t) and U_t and U_x are both used in the equation. It is a first-order equation because only first derivatives appear. Equations (A.2a) and (A. 2b) are nonlinear because the unknown variable, or dependent variable, U, is multiplied by itself or its derivatives. Burgers equation belongs to a special class of nonlinear equations called quasi-linear equations. A quasi-linear equation is one in which the highest order derivatives appear to the first power, as is most easily seen in Equation (A.2b). The three-dimensional Euler equations of inviscid fluid flow are another example of quasi-linear equations.

To provide a good test case for the finite volume approaches, we need to know some exact solutions to Burgers equation. First, solve Equation (A.2) with the general initial conditions,

$$U(x,0) = f(x). \qquad (A.3)$$

The solution to the problem will be of the form U=g(x,t). Now consider a three-dimensional space with x,t, and U coordinate axes, and define

$$0 = U - g(x,t). \qquad (A.4)$$

The surface $\phi(x,t,U)=0$ in the three-dimensional space defines the solution to the problem. In other words, any point on the surface, say x_o, t_o, U_o is a point of the solution given by $U(x_o,t_o)= U_o$. A vector perpendicular to the surface is given by grad $\phi = (\phi_x, \phi_y, \phi_z)$, and any vector perpendicular to grad ϕ must be tangent to the solution surface. If (x_o, t_o, U_o) is a point of the solution, and, for infinitesimal displacements, (x_o+dx, t_o+dt, U_o+du) is also a point of the solution, then

$$\text{grad } \phi \cdot dx = 0,$$

or
$$\phi_x dx + \phi_t dt + \phi_U du = 0. \tag{A.5}$$

Using Equation (A.4) in Equation (A.5)

$$-g_x - g_t + du = 0. \tag{A.6}$$

6. From Equation (A.2) the following results when $U= g(x,t)$,

$$g_t + Ug_x = 0,$$

from which we can tell that if we take dx, dt, and du in the following ratios, Equation (A.6) will be satisfied:

$$dt/1 = dx/U = du/0. \tag{A.7}$$

If r is taken as a parameter along the solution curve, then Equation (A.7) can be written:

$$dt/dr = 1 \ , \ dx/dr = U \ , \ du/dr = 0; \tag{A.8}$$

with the initial conditions:

$$t = 0 \ , \ x = x_o \ , \ U = f(x_o).$$

Solving these equations gives

$$t(r) = r \ , \ U(r) = \text{constant} = f(x_o) \text{ and}$$

dx/dr gives

$$x(r) = rf(x_o) + \text{constant and } x(0) = \text{constant} = x_o.$$

Therefore;

$$x(r) = rf(x_o) + x_o$$
$$x(t) = tf(x_o) + x_o.$$

For an example, take

$$f(x) = \begin{cases} 1 & , \ x \leq 0 \\ 1-x & , \ 0 \leq x \leq 1 \\ 0 & , \ x \geq 1 \end{cases}$$

1.) For $x_o \geq 1$ (Figure A-1);

$$x(t) = tf(x_o) + x_o = x_o$$
$$U(r) = f(x_o) = 0$$
$$U(x,t) = 0.$$

2.) For $x_o \leq 0$ (Figure A-1);

$$x(t) = t + x_o$$
$$U(r) = f(x_o) = 1$$
$$U(t+x_o,t) = 1$$

since $x_o = x-t$ when $U(x,t) = 1$.

3.) For $0 \leq x \leq 1$ (Figure A-1);

$$x_o = (x-t)/(1-t)$$
$$U(x,t) = (1-x)/(1-t).$$

This method of characteristics analysis shows the Burgers equation capability to produce shocks or discontinuities in the flow field. This capability allows one to test numerical shock-capturing methods using the inviscid Burgers equation and apply them to the three-dimensional Euler equations for inviscid fluid flow.

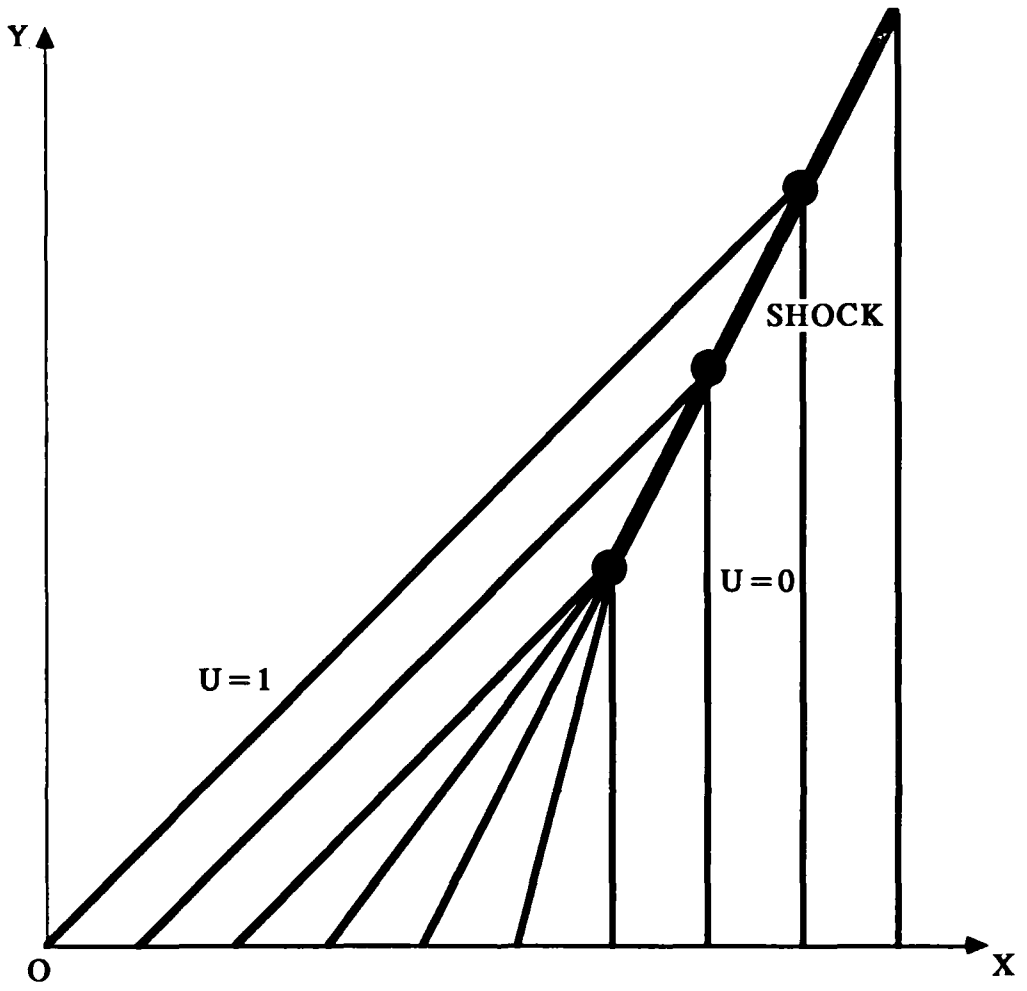

Figure A-1. Characteristic Solution to the Inviscid Burgers Equation

APPENDIX B

ANALYSIS OF NUMERICAL TECHNIQUE

This section of the analysis examines the numerical characteristics of the Warming-Beam algorithm for the general finite-difference approach (References 1 and 2). Finite-difference methods involve approximating the continuous domain of any problem by a discrete domain (grid) and approximating the PDE's governing any problem by one or more algebraic or finite difference equations (FDE's). The total error in the solutions of FDE's is made up of discretization error and stability error. Stability error is small for stable FDE's since by definition disturbances and errors cannot grow. Therefore, discretization error accounts for most of the total error. The discretization error is made up of dissipation and dispersion error.

For this examination the governing PDE is the inviscid Burgers equation:

$$U_t + (U^2/2)_x = 0 \ . \tag{B.1}$$

To determine if a FDE is an algebraic analog of a PDE,and is agood approximation of the exact solution of the PDE, we must involve the concepts of consistency, numerical stability, convergence, phase and dispersion error, and artificial dissipation (Reference 3).

1. LINEARIZATION

For the purpose of linear stability theory, we employ a linearization method to the nonlinear PDE,

$$U_t + UU_x = 0.$$

The resulting linearized PDE is the convection or linear wave equation:

$$U_t + CU_x = 0, \tag{B.2}$$

and, for continuity, the linear equation will be used throughout the FDE analysis.

Locally, the PDE may be approximated by the linear PDE with constant coefficients even though the PDE is globally nonlinear. This approach yields reasonable results; however, the resulting stability criteria (to be discussed in more detail in subsection 3) is necessary, but not sufficient. The resulting Warming-Beam upwind scheme for the linear wave equation is as follows:

Predictor:
$$\frac{U_i^{n+1} - U_i^n}{\Delta t} + C\,\frac{U_i^n - U_{i-1}^n}{\Delta x} = 0 \tag{B.3a}$$

$$\text{Corrector:} \quad \frac{U_i^{n+1} - 1/2\,(U_i^{n+1} + U_i^{n})}{\frac{\Delta t}{2}} + C\,\frac{U_i^{n+1} - U_{i-1}^{n+1}}{\Delta x} =$$

$$-C\,\frac{U_i^{n} - 2U_{i-1}^{n} + U_{i-2}^{n}}{\Delta x} \qquad \text{(B.3b)}$$

2. CONSISTENCY

To analyze the consistency of the FDE (Equation B.3a,b) used to model the PDE (Equation B.2), we must express U_i^{n+2}, U_i^{n+1}, U_i^n in terms of U_i^n and its derivatives by using a Taylor series expansion:

$$U_i^{n+1} = U_i^n + U_i^{i}\,\Delta t + U_i^{"}\frac{\Delta t^2}{2!} + U_i^{"'}\frac{\Delta t^3}{3!} + \cdots \qquad \text{(B.4a)}$$

$$U_i^{n+2} = U_i^n + U_i^{i}\,2\Delta t + U_i^{"}\frac{4\Delta t^2}{2!} + U_i^{"'}\frac{8\Delta t^3}{3!} + \cdots \qquad \text{(B.4b)}$$

$$U_{i-1}^{n} = U_i^n - U_i^{i}\,t + U_i^{"}\frac{\Delta t^2}{2!} - U_i^{"'}\frac{\Delta t^3}{3!} + \cdots \qquad \text{(B.4c)}$$

The reason for this is that the FDE was derived by applying the PDE at grid point i and time level n. Substituting the expansions into the FDE yields

$$U_t + CU_x = O\,(\Delta x^2, \Delta x\,\Delta t, \Delta t^2), \qquad \text{(B.5)}$$

therefore, Equation (B.5) is mathematically equivalent to the PDE as the grid spacing (Δ x) and time-step size (Δ t) approach zero.

An FDE is consistent if for every i and n;

$$\lim_{\substack{\Delta x \to 0 \\ \Delta t \to 0}} \text{FDE} = \text{PDE} \qquad \text{(B.6)}$$

Consistency measures the extent to which an FDE approximates a PDE in some limiting case. A consistency analysis was performed on the upwind scheme and it was found that the upwind scheme, when applied to the convection equation, is unconditionally consistent. This means that the

$$\lim_{\substack{\Delta t \to 0 \\ \Delta x \to 0}} (FDE)_i^n = (PDE)_i^n \qquad \text{(B.7)}$$

regardless of how x and t approach zero. Terms such as $\Delta\ tU_i^n$ or $\Delta\ xU_i^n$ can be added to the FDE and the resulting FDE will remain unconditionally consistent; therefore, there are an infinite number of unconditionally consistent FDE's for a given PDE. Consistency alone, however, will not guarantee the accuracy of the solutions of the FDE's since all computations are performed by using finite $\Delta\ x$ and $\Delta\ t$.

3. STABILITY

Numerical stability is concerned with how errors propagate as the solution is advanced in a time-like variable, and is a concept applicable only to parabolic and hyperbolic PDE's. An FDE is stable if the stability error approaches zero or does not grow. A given FDE may yield stable or unstable numerical solutions depending upon the value of some dimensionless parameter ($\nu = c\ \Delta t/\Delta x$). The need to obtain stable numerical solutions is critical to the solution of a given PDE since only stable numerical results have a chance of being physically meaningful. Conditionally stable FDE's are those that yield stable solutions when Δx and Δt are in a given form ($\nu = c\Delta t/\Delta x$). Unconditionally stable FDE's are those that give stable solutions for any Δx and Δt. Unconditionally unstable FDE's give unstable solutions for every Δx and Δt. Typically, stability bounds for implicit methods are less restrictive than those for explicit methods .

There are many different mathematical methods for analyzing the numerical stability of FDE's. For this examination, the Von Neumann or Fourier method is employed. In the Fourier method, the numerical stability of an FDE is analyzed by introducing a disturbance into the numerical solution at every grid point in the spatial domain at some arbitrary time level. The disturbance is expanded into a Fourier series and each Fourier component of that series is analyzed separately. The FDE is stable if all of the Fourier components do not grow in time and unstable if any one of the Fourier components grows in time. The method of analyzing each Fourier component separately is valid only when the FDE's are linear with respect to the dependent variable. For this examination the FDE is not linear and must be linearized before the stability property can be determined.

A Fourier stability analysis has been performed on the upwind scheme using the linear wave equation. Results show that it is conditionally stable with the following conditions:

$$0 \leq \nu = c\ \Delta t/\Delta\ x \leq 2 \qquad \text{(B.8)}$$

4. CONVERGENCE

An FDE is convergent if the numerical solution of the FDE approaches the exact solution of the PDE as the time-step size and grid spacing approach

zero. A convergent FDE can yield a solution of any desired accuracy by reducing the time-step size (Δ t) and the grid spacing (Δ x). The analysis of the convergence of an FDE for a complex PDE is extremely difficult, and convergence analysis techniques are only available for linear PDE's.

The convergence analysis has been performed for the upwind scheme with respect to the linear wave equation and results show the FDE to be convergent (Reference 1).

If the FDE is well-posed, consistent, and stable (as is the case in this examination); the Lax Equivalence Theorem states that the FDE of the linear PDE is convergent. Therefore, according to this theorem, the Warming-Beam upwind scheme should be convergent. For FDE's of quasi-linear and nonlinear PDE's, the Lax Equivalence Theorem serves as an important guideline; hence, consistency and stability are crucial tests for convergence.

5. MODIFIED EQUATION

In the modified equation analysis, a PDE is derived that is mathematically equivalent to the FDE to be examined. The resulting PDE is called the modified equation.

The modified equation is derived by the following two-step procedure:

(1) Expand each term in the FDE in a Taylor series expansion.

(2) Express all time derivatives (with the exception of the first-order time derivative) in terms of spatial derivatives.

The modified equation for this examination is given by

$$U_t+CU_x = (c\Delta x^2/6)\ (1-\nu)\ (2-\nu)\ U_{xxx} - (\ x^4/8\Delta t)\nu\ (1-\nu)^2(2-\nu)\ U_{xxxx}+\ldots(B.9)$$

This method of analysis is used exclusively in support of the dissipation and dispersion error investigations.

6. PHASE AND DISPERSION ERROR

Dispersion is mathematically described by the odd-order spatial derivatives. The coefficients of the odd-order spatial derivatives in the modified equation for the FDE must be identical to the corresponding coefficients in the PDE in order for a FDE to have the same dispersive characteristics as the PDE it is to represent. If the corresponding coefficients are different, then the solutions of the FDE's contain dispersion errors. Since the coefficients of the odd-order spatial derivatives in the modified equation do not match the corresponding coefficients in the PDE, the FDE contains dispersion error. The order of dispersion is equal to the order of

the coefficients of the lowest odd-order spatial derivative excluding the first order spatial derivative. Therefore, the FDE contains second-order dispersion; the higher the order of dispersion, the lower the dispersion error.

$$U_t + CU_x = 0$$

$$U_t + CU_x - (c\Delta x^2/6)\ (1-\nu)\ (2-\nu)\ U_{xxx} + (\Delta x^4/8\Delta t)\ \nu(^1\ \nu)^2(2-\nu)\ U_{xxxx} + \cdots = 0$$

The dispersion error is examined by the Von Neumann method (Reference 1). The dispersion error for each Fourier component of a disturbance after n time steps is given by

$$n(\emptyset pde - \emptyset fde) \tag{B.10}$$

where

Opde = phase angle of the amplification factor (PDE)

Ofde = phase angle of the amplification factor (FDE)

The dispersion error after n time steps, for this analysis, is given by

$$n\left\{-\gamma\nu - \tan^{-1}\left[\frac{1-2\nu\ \ (\nu+2\ (1-\nu)\ \sin^2\frac{\gamma}{2})\ \sin^2\frac{\gamma}{2}}{\nu\sin\gamma(1+2\ (1-\nu)\ \sin^2\frac{\gamma}{2})}\right]\right\} \tag{B.11}$$

The relative phase shift error for a given Fourier component after one time step is

$$Ofde\ /\ \ Opde \tag{B.12}$$

The relative phase shift error for this examination is

$$\tan^{-1}\left[\frac{1-2\ \nu(\nu+2\ (1-\nu)\ \sin^2\frac{\gamma}{2})\ \sin^2\frac{\gamma}{2}}{\nu\sin\gamma\ (1+2\ (1-\nu)\ \sin^2\frac{\gamma}{2})}\right] \tag{B.13}$$

$$-\gamma\nu$$

The dispersion error is given by these two relationships because the phase angle of the amplification factor depends only on the odd-order spatial derivatives when the highest time derivative is first-order.

For leading phase error, the relative phase shift error must be greater than unity for a given Fourier component (the numerical solution for that Fourier component gives a wave speed greater than the wave speed given by the exact solution). Lagging phase error results when the relative phase shift error is less than unity for a given Fourier component (the numerical solution for that Fourier component gives a wave speed less than the wave speed given by the exact solution).

The Warming-Beam upwind scheme, with respect to the convection equation, has a lagging phase error when ν is greater than one and a predominantly

leading phase error when is less than one. When ν does not equal one, the relative phase shift error increases as the wave number, γ $(K_j \Delta x)$, increases (Figure B-1).

7. ARTIFICIAL DISSIPATION

As diffusion spreads a disturbance in every direction, the disturbance is smoothed out over an increasingly large area. Diffusion reduces spatial gradients and lowers the magnitude of the disturbance by spreading it out; this phenomenon is termed dissipation. Diffusion is mathematically described by even-order spatial derivatives in a PDE; if the even-order spatial derivatives in the PDE are zero, the PDE will not have any dissipation.

In order for a FDE to have the same dissipative characteristics as that of the PDE it is modeling, the coefficients of the even-order spatial derivatives in the modified equation for the FDE must be identical to the corresponding coefficients of the PDE. The PDE for our examination is, again,

$$U_t + CU_x = 0$$

The modified equation for the upwind scheme is given by (Equationf B.9)

$$U_t + CU_x = (c\Delta x^2/6)\ (1-\nu)\ (2-\nu)\ U_{xxx} + (\Delta x^4/8\Delta t)\nu\ (1-\nu)^2(2-\nu)\ U_{xxxx} + \cdots$$

Therefore, since the corresponding even-order coefficients are not identical, there is fourth-order dissipation error in the solution of the FDE.

The dissipation error is examined using the Von Neumann method. The dissipation error for each Fourier component of a disturbance after n time steps is

$$(\ G^n_{pde} - G^n_{fde})\ A^o, \qquad \text{(B.14)}$$

G_{pde} = amplification factor (PDE)

G_{fde} = amplification factor (FDE)

A^o = initial amplitude of the Fourier component

The dissipation error is given by this relationship because the modulus of the amplification factor depends on the even-order spatial derivatives when the highest time-derivative is first-order.

The dissipation error, for this examination, for a given time-step, n, is given by

$$1- \left[\ (1-4\ \nu(1-\nu)^2\ (2-\nu)\ \sin^4\frac{\gamma}{2})^{1/2}\ \right]^n \qquad \text{(B.15)}$$

For values of ν less than one, as decreases, the dissipation error increases, and for values of ν greater than one, as ν increases, the dissipation error inccreases. Also, for values of ν not equal to unity, as the wave number, γ $(k_j\ \Delta\ x\ )$, increases the dissipation error increases (Figure B-2).

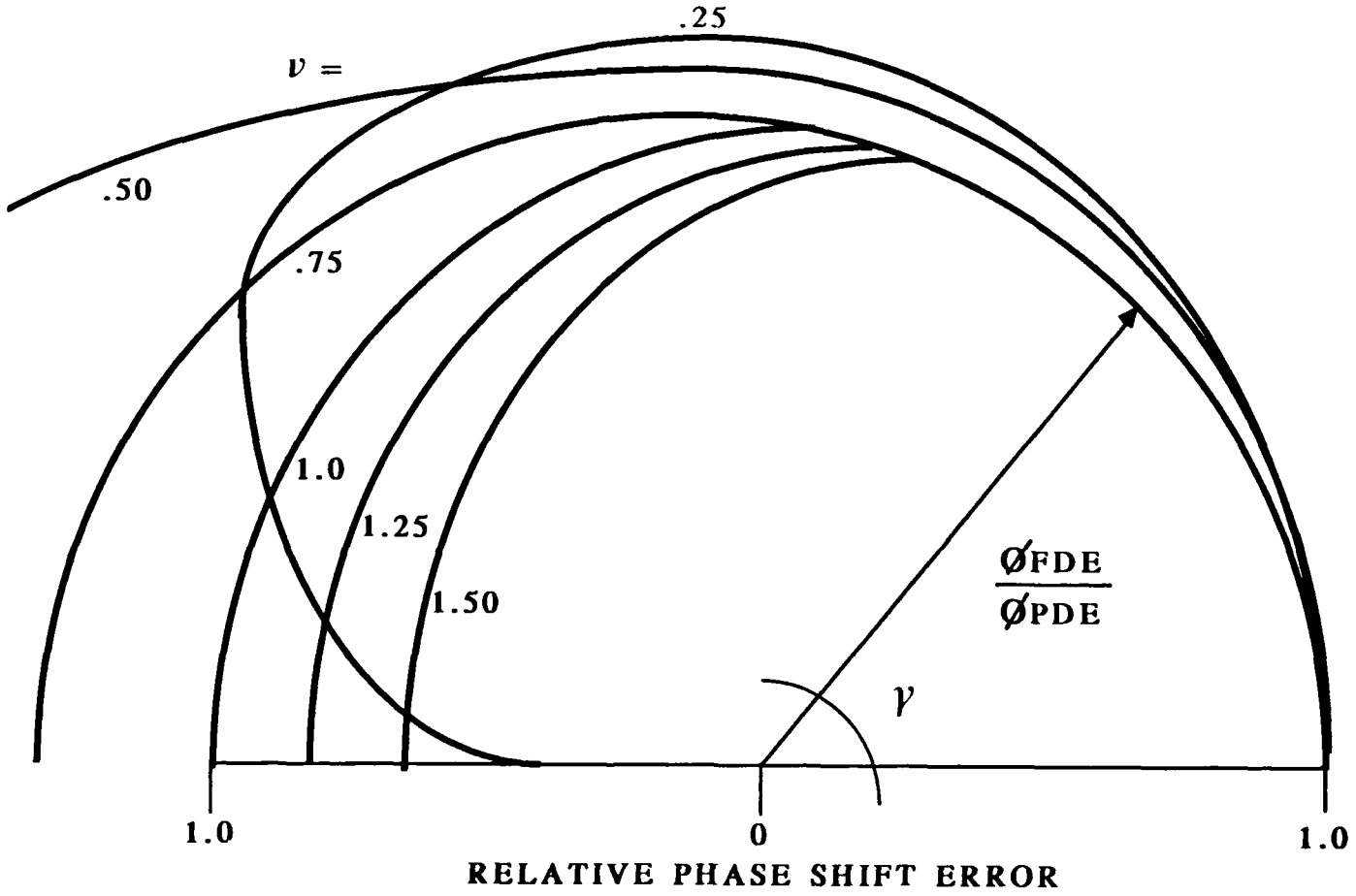

Figure B-1. Relative Phase Shift Error $\frac{\text{ØFOE}}{\text{ØPDE}}$ vs Courant Number (ν)

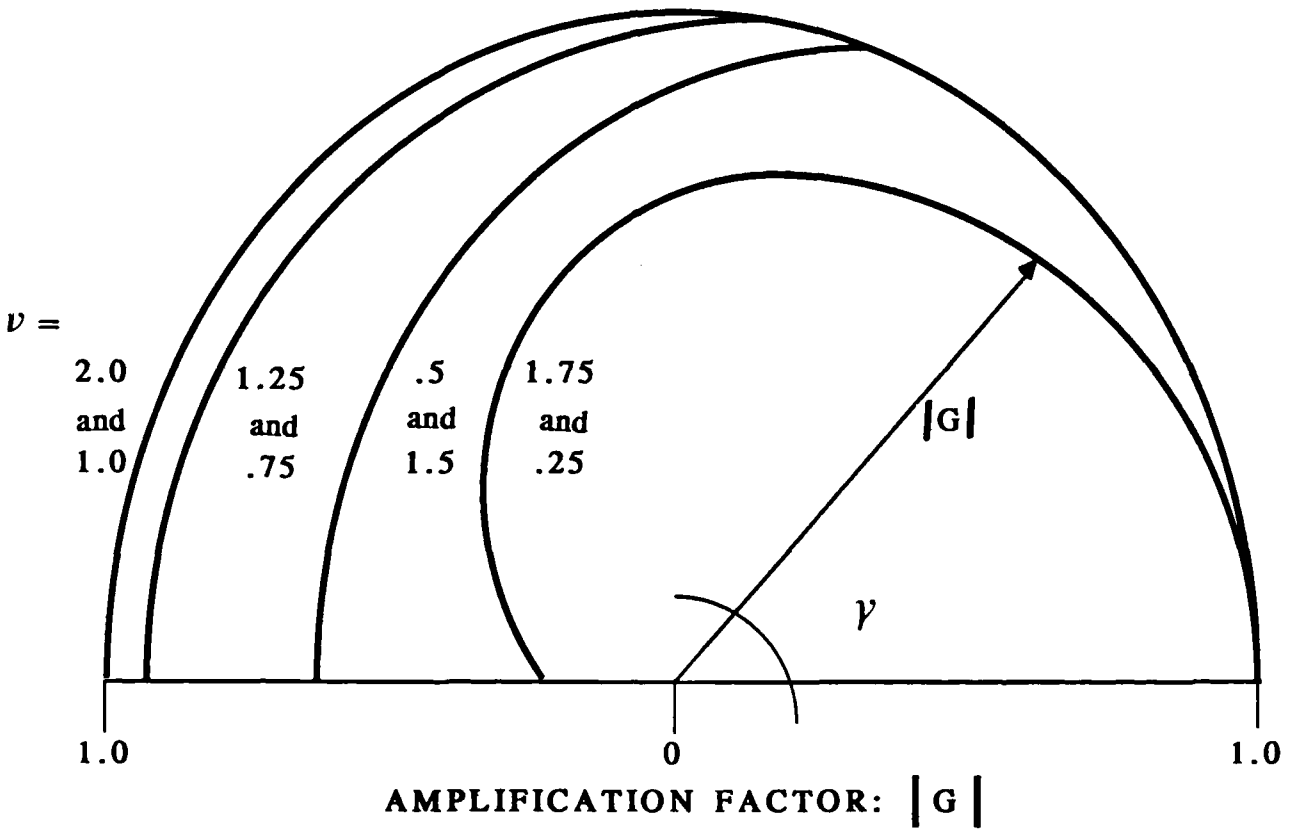

Figure B-2. Amplification Factor Modulus -|G| vs Courant Number (ν)

REFERENCES

1. D.A. Anderson, J.C. Tannehill, and R.H. Pletcher, Computational Fluid Mechanics and Heat Transfer., McGraw-Hill Book Co., New York, 1984.

2. R.F. Warming and R.M. Beam. "Upwind Second-Order Difference Schemes and Applications in Unsteady Aerodynamic Flows," Proc. AIAA 2nd Computational Fluid Dynamics Conference, Hartford, Conn., 1975,

3. T. I-P. Shih, Finite-Difference Methods in Computational Fluid Dynamics, to be published by Prentice-Hall Pub.

4. D.L. Whitfield and J.M. Janus, "Three-Dimensional Unsteady Euler Equations Solution Using Flux Vector Splitting," AIAA-84-1552, Jun 1984.

5. W. Schmidt, A. Jameson, and D.L. Whitfield, "Finite Volume Solution for the Euler Equation for Transonic Flow over Airfoils and Wings Including Viscous Effects," AIAA-81-1265, Ca., Jun 1981.

6. D.M. Belk, J.M. Janus, and D.L. Whitfield, "Three-Dimensional Unsteady Euler Equations Solutions on Dynamic Grids," AIAA-85-1704, Apr 86.

INITIAL DISTRIBUTION

DTIC-DDAC	2
AUL/LSE	1
FTD/SDNF	1
HQ USAFE/INATW	1
AFWAL/FIES/SURVIAC	1
AFATL/DOIL	2
AFATL/CC	1
AFCSA/SAMI	1
AFATL/CCN	1
AFATL/FXA	10
AFATL/FX	2
USAFA/DFAN	1
USAFA/DFAN (PERSONNEL)	1
AD/YHP	1
AFATL/MN	1
AD/TYD	1
AFOSR/NA	1
NASA AMES RT	1

END

2-87

DTIC